UNCLASSIFIED

ORNL 366
PHYSICS-GENERAL

MARTIN MARIETTA ENERGY SYSTEMS LIBRARIES
3 4456 0050898 4

PHYSICS DIVISION

PROGRESS REPORT FOR THE QUARTER ENDING

JUNE 15,1949

A.H. SNELL, DIRECTOR
E.O. WOLLAN, ASSOCIATE DIRECTOR

CENTRAL RESEARCH LIBRARY
DOCUMENT COLLECTION

LIBRARY LOAN COPY

DO NOT TRANSFER TO ANOTHER PERSON

If you wish someone else to see this document, send in name with document and the library will arrange a loan.

OAK RIDGE NATIONAL LABORATORY

OPERATED BY
CARBIDE AND CARBON CHEMICALS CORPORATION
FOR THE
ATOMIC ENERGY COMMISSION
POST OFFICE BOX P
OAK RIDGE, TENNESSEE

UNCLASSIFIED

UNCLASSIFIED

ORNL 366
Copy No. 7

Contract No. W-7405, eng 26

PHYSICS DIVISION
PROGRESS REPORT FOR THE QUARTER ENDING
JUNE 15, 1949

A. H. Snell, *Director*

E. O. Wollan, *Associate Director*

AUG 1 2 1949

OAK RIDGE NATIONAL LABORATORY

operated by
CARBIDE AND CARBON CHEMICALS CORPORATION
for the
ATOMIC ENERGY COMMISSION
Post Office Box P
Oak Ridge, Tennessee

MARTIN MARIETTA ENERGY SYSTEMS LIBRARIES
3 4456 0050898 4

UNCLASSIFIED

ORNL 366 Supplement 1
Physics-General

OAK RIDGE NATIONAL LABORATORY INTERNAL DISTRIBUTION:

1. G. T. Felbeck (C&CCC)
2-3. 706-A Library
4. 706-B Library
5. Biology Library
6. Health Physics Library
7-8. Training School Library
9-12. Central Files
13. J. A. Swartout
14. J. H. Gillette
15. A. Hollaender
16. J. H. Frye, Jr.
17. E. J. Murphy
18. M. D. Peterson
19. C. N. Rucker
20. W. D. Lavers
21. A. M. Weinberg
22. J. S. Felton
23. A. H. Snell
24. E. O. Wollan
25. K. Z. Morgan
26. G. E. Boyd
27. Lewis Nelson
28. R. W. Stoughton
29. J. A. Lane
30. M. M. Mann
31. A. Householder
32. C. E. Winters
33. E. P. Blizard
34. W. H. Jordan
35. F. C. VonderLage
36. Central Files (Off-Plant)

OAK RIDGE NATIONAL LABORATORY EXTERNAL DISTRIBUTION:

37-48. Argonne National Laboratory
49. Armed Forces Special Weapons Project
50-51. Atomic Energy Commission, Washington
52. Battelle Memorial Institute
53-56. Brookhaven National Laboratory
57. Bureau of Ships
58-61. Carbide and Carbon Chemicals Corporation (K-25 Plant)
62-65. Carbide and Carbon Chemicals Corporation (Y-12 Plant)
66. Columbia University (Dunning)
67-70. General Electric Company, Richland
71. Hanford Operations Office
72. Iowa State College
73-74. Kellex Corporation
75-78. Knolls Atomic Power Laboratory
79-81. Los Alamos
82-84. Mound Laboratory
85. National Advisory Committee for Aeronautics
86-87. National Bureau of Standards
88. Naval Radiological Defense Laboratory
89. NEPA Project
90. New Brunswick Laboratory
91-92. New York Operations Office
93. North American Aviation, Inc.
94. Patent Branch, Washington
95. Sandia Laboratory
96-110. Technical Information Branch, ORE
111. UCLA Medical Research Laboratory (Warren)
112-116. University of California Radiation Laboratory
117-118. University of Rochester
119-122. Westinghouse Electric Corporation

TABLE OF CONTENTS

SUMMARY 5

PHYSICAL ELECTRONICS

Scintillation Spectrometer 7

High Speed Oscilloscope 24

Short-Lived Isomers 29

SEMI-CONDUCTORS 36

NUCLEAR PHYSICS AND NEUTRON DIFFRACTION

Scattering by Paramagnetic and Antiferromagnetic Materials 38

Neutron-Proton Scattering 41

Growing Large Crystals of Copper-Gold Alloy 42

Neutron Activation Studies with Fast Pneumatic Tube 43

Cadmium Capture γ-Rays 43

Pile Oscillator 43

NUCLEAR PHYSICS AND LOW TEMPERATURES

Low Temperature Program 48

Cross Section of He^3 as a Function of Energy 48

VAN DE GRAAFF 50

SHIELDING 53

THEORETICAL PHYSICS 54

NEUTRON DECAY 55

SUMMARY

Scintillation Counting. One of the principal events of the past quarter was a two-day Symposium on Scintillation Counting, organized mainly by W. H. Jordan, at which about 125 visitors from various parts of the continent attended. Dr. Martin Deutsch acted as guest chairman, and the principal speakers were H. Kallmann, F. Seitz, G. A Morton, and P. R. Bell.

In this Quarterly Report, P. R. Bell describes the following observations made with his scintillation counter, which is used as a spectrometer of high intensity and rather good resolution:

(1) Beta spectra of P^{32}, Y^{91}, and Cs^{137} are given, together with Kurie plots. Agreement with beta spectrometer results is good.

(2) The beta spectrum of Be^{10} is found to correspond to a forbidden transition.

(3) Beta rays are found to accompany the 4.5 hr isomeric transition in In^{115}.

High-speed Oscilloscope. This instrument (rise time 5×10^{-9} sec) has been used to obtain some very beautiful and instructive pictures of the groups of pulses obtained from several phosphors useful for scintillation counting. Phenanthrene was found to be fastest, with a decay constant of 0.008 μ sec.

Short-lived Isomers. Four radioactive isotopes reported last quarter as possibly having short-lived isomeric states have been found on closer examination not to have them. Existence of an isomeric state in Cd^{111} has been confirmed, and the associated half-life has been measured as $9 \pm 1 \times 10^{-8}$ sec. Nineteen other radioactive isotopes have given negative results.

Neutron Diffraction. Work continues on magnetic scattering in manganese compounds. At 80° K, MnO gives strong coherent magnetic scattering which is not present at room temperature, and which apparently originates from unit cells with edges double the length of the chemical unit cell.

Refinements are being introduced into the measurement of the coherent scattering of neutrons by hydrogen in NaH, in order to check older values of the range of the neutron-proton interaction.

Low Temperatures. An electromagnet for adiabatic demagnetization has been built and installed. Studies are being made concerning heat flow to the crystal of refrigerating salt from a copper or silver bar which will eventually be attached to the specimen to be cooled.

Pile Oscillator. The capture cross section of 69 elements are summarized.

Capture Gamma Rays of Cadmium. Final results are given of the cloud chamber study of pairs produced by the gamma rays produced by neutron capture is cadmium.

Short-Period Activities. A new activity with half-life of about 1 sec has been found in lead. Pb^{205} is not responsible, and studies as to the characterization and identification of the activity are continuing.

Neutron Decay. Fairly convincing coincidence results indicate that neutrons decay radioactively with a half-life between 10 and 30 minutes.

Shielding. Work continues on the technique of measuring high-energy gamma rays by means of deuterium-loaded photographic emulsions.

A summer session has been organized for study and evaluation of the present state of the whole shielding problem.

Irradiation of Semi-Conductors. Transmutation by slow neutron capture has been found sufficient to account for all of the impurity centers found by Hall effect measurements to have been introduced by pile irradiation of germanium.

Van de Graaff Program. The 2 Mev machine has been installed in the old Laboratory heating plant. Work on conversion of this machine into a positive ion accelerator continues, with development of the ion source, the accelerating tube, and schemes for differential pumping at the high voltage end.

Theoretical Physics. Preparations are being made to extend the K-shell internal conversion coefficient calculations to the L-shell. This promises to be a major computational task.

PHYSICAL ELECTRONICS

Scintillation Spectrometer (P. R. Bell, J. M. Cassidy and R. C. Davis). The proportionality previously found between the photomultiplier pulse of a scintillation counter and the energy of the electron (β-ray or Compton electron) entering the phosphor has been exploited to such an extent that the instrument using this effect has been termed a scintillation spectrometer. By cataloging the pulses according to height, a spectrum of the impinging radiation is obtained.

The instrument has been used to investigate the β-spectrum of Be^{10}; it has also been used to show that In^{115*}, formerly thought to decay only to the ground state of In^{115} by emission of a partially internally converted gamma ray, actually decays also by β-ray emission to Sn^{115}. The following curves serve to show the performance of the instrument and some of the results obtained.

Figure 1 is a block diagram of the equipment. An anthracene crystal ~1.5 in. diameter, 0.5 in. thick is cemented to the end of an RCA C-7132 photomultiplier with Canada balsam and covered with a thin aluminum foil light reflector. The sources, prepared as for a magnetic β-ray spectrometer, are placed near the crystal. If γ-rays must be determined also, space must be left for an absorber thick enough to stop all β-rays or conversion electrons from the source. The source, crystal and tube are enclosed in a light tight box of thick plastic to reduce bremstrahlung pulses. The rest of the block diagram is self explanatory.

Figure 2 shows the pulse height-number curve produced by the gamma rays of Na^{24}. This is the curve of the number of pulses whose height lies between E and E + ΔE, plotted against the pulse height E. The width of the interval ΔE is about 30 units on the pulse height selector scale.

The lower curve with the two peaks represents the derivative of the pulse height-number curve and the peaks represent the maximum energy of Compton electrons from each γ-ray. The energy of the gamma ray is found from the usual Compton formula

$$\frac{E_e}{E_\gamma} = \frac{1}{1 + \frac{E_o}{2E_\gamma}}$$

where E_e = maximum energy of Compton electrons,

E_γ = energy of gamma rays,

and E_o = self energy of an electron, 0.511 Mev.

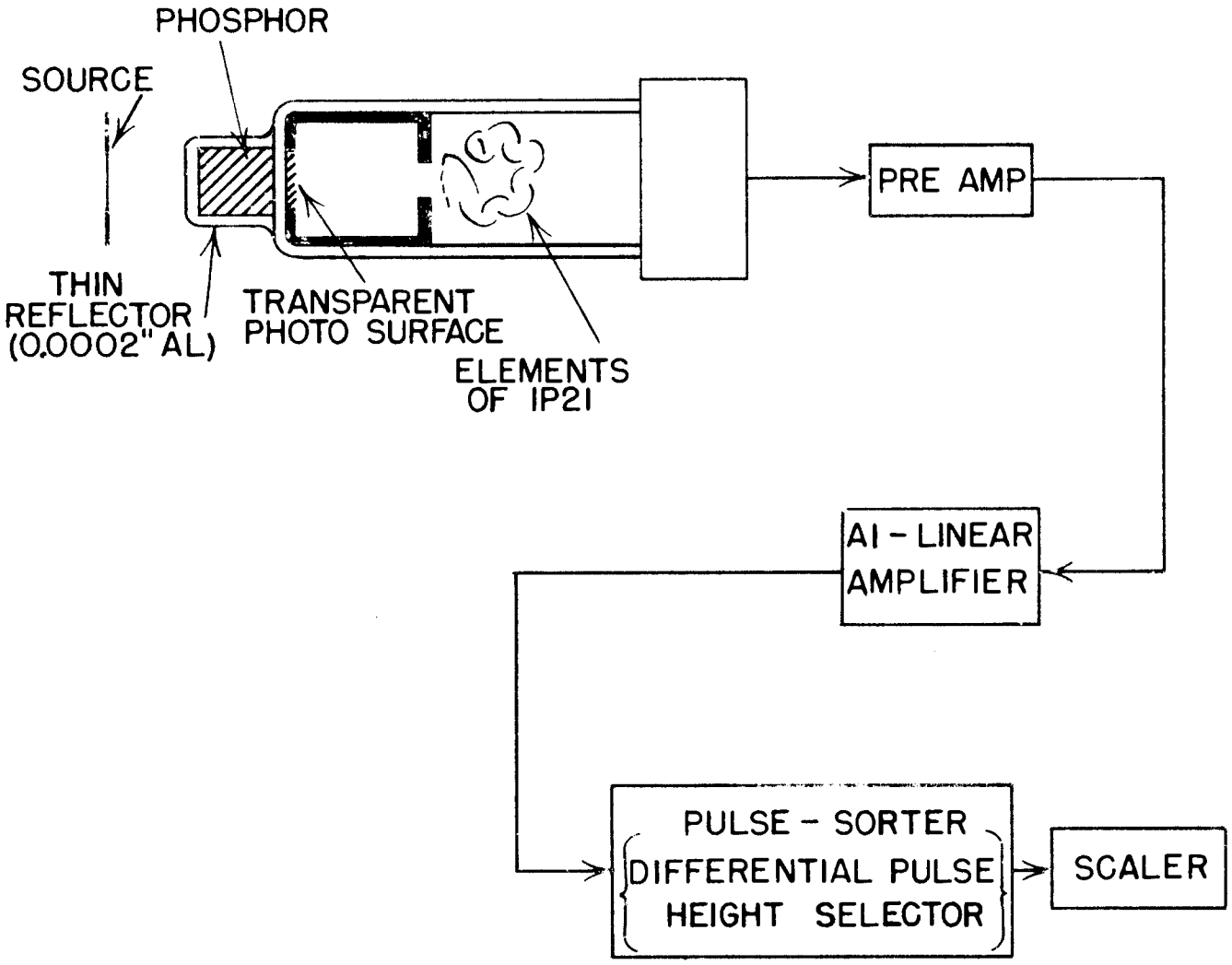

FIG. 1
SCINTILLATION SPECTROMETER

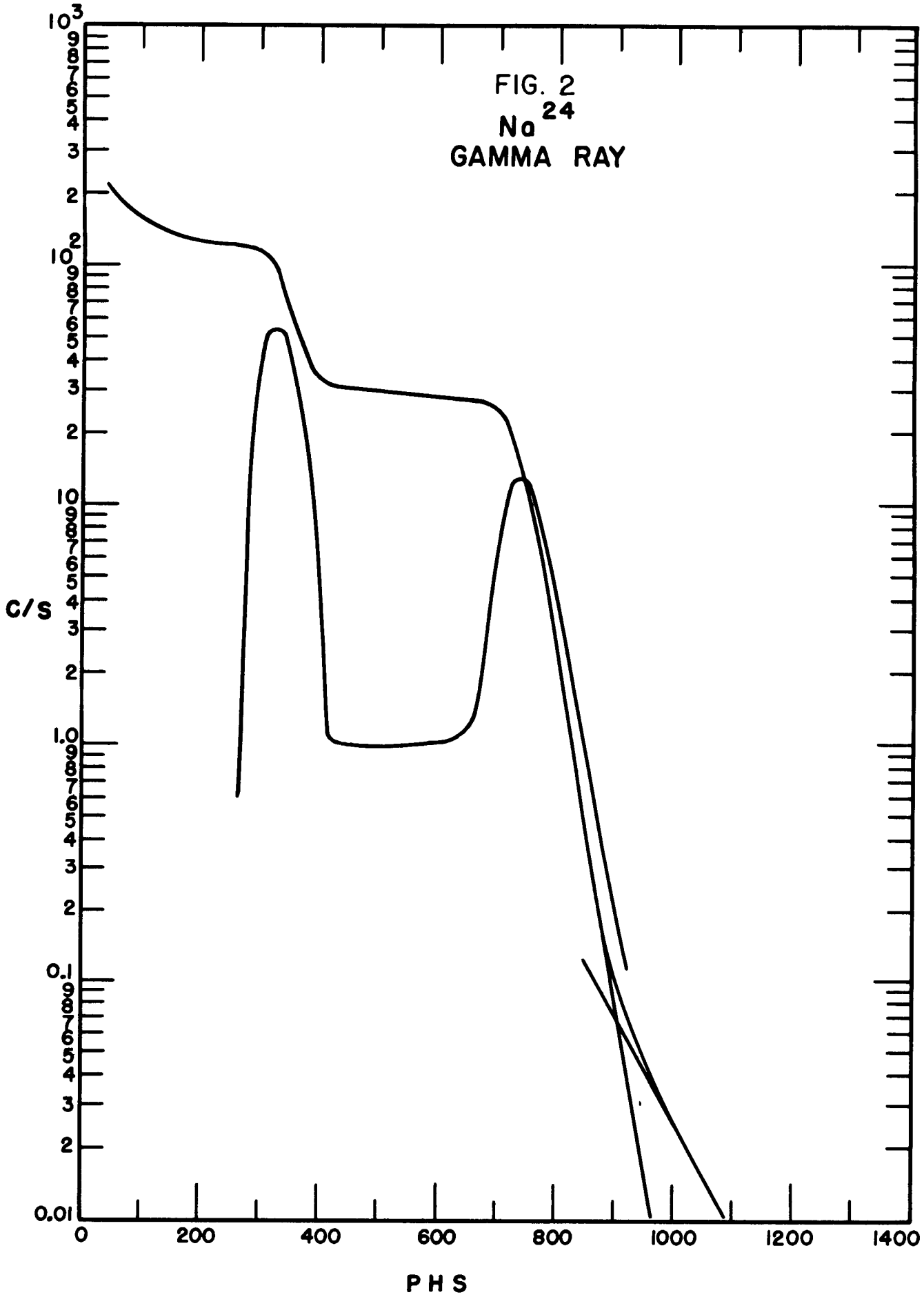
FIG. 2
Na 24
GAMMA RAY
C/S
PHS
0.01
0.1
1.0
10
10 2
10 3
0
200
400
600
800
1000
1200
1400

The out-curving foot of the pulse height-number curve was examined to see if a cross-over gamma ray was present. It appears to be due mostly or entirely to accidental coincidences between pulses. The resolution time of the equipment was set at 1.0 microsecond and the total counting rate was 2-5 thousand pulses per second. The cross-over gamma ray, if present, must be less than 1/1000 the intensity of either lower gamma ray.

Figure 3 shows a similar set of curves for the Zn^{65} gamma ray. The efficiency of this crystal has not yet been measured at many energies (work in progress), but its efficiency at the energy of the Cs^{137} gamma ray (0.67 Mev) is 13%. By this we mean that 13% of all 0.67 Mev gamma rays passing through the crystal produce pulses that are counted.

Many beta ray emitters have been measured on the equipment, and the Kurie plots produced for P^{32} and Y^{91} are shown in Fig. 4. The pulse height scale was calibrated in energy units by the conversion line from Cs^{137} at 630 kev. The departure from a straight line for P^{32} is partly due to scattering out of beta rays from the crystal before all of their energy has been lost. A second cause for the excess of small pulses is the variation of the pulse height selector *window* (ΔE) with pulse height selector setting. The window becomes wider at lower settings.

The data have been corrected for the poor resolution of the instrument by the method of Primakoff and Owen[1]. This correction has negligible effect except near the upper end of the spectrum, and there it removes a turn out seen in many Kurie plots from other β-ray spectrometers, and especially prominent in this one.

The Kurie plot for Y^{91} is much more curved and is actually the 1st forbidden tensor or axial vector shape with spin change 2. The lower curve is also for Y^{91} but the factor a, $(p^2 + q^2)$, has been used and the plot is about as straight as for P^{32}. The forbidden shape of the Y^{91} spectrum was apparently discovered simultaneously by many workers independently and was called to our attention by B. Ketelle of the Chemistry Division.

Figure 5 shows the Cs^{137} spectrum which was used as a calibration for the Be^{10} data. The "γ only" curve was subtracted from the gross counts to get the "γ subtracted" curve which is the spectrum due to electrons only. The conversion peak at 630 kev can be seen as well as the lower β-ray (maximum energy 0.5 Mev) and the upper β-ray (maximum energy 1.2 Mev)[2]. A Kurie plot of the lower β-ray was obtained by assuming the conversion peak to be symmetrical and

[1] G. E. Owen, H. Primakoff, *Phys. Rev.*, **74**, 1406 (1948).

[2] Peacock, Mitchell, *Phys. Rev.*, **75**, 1272 (1949).

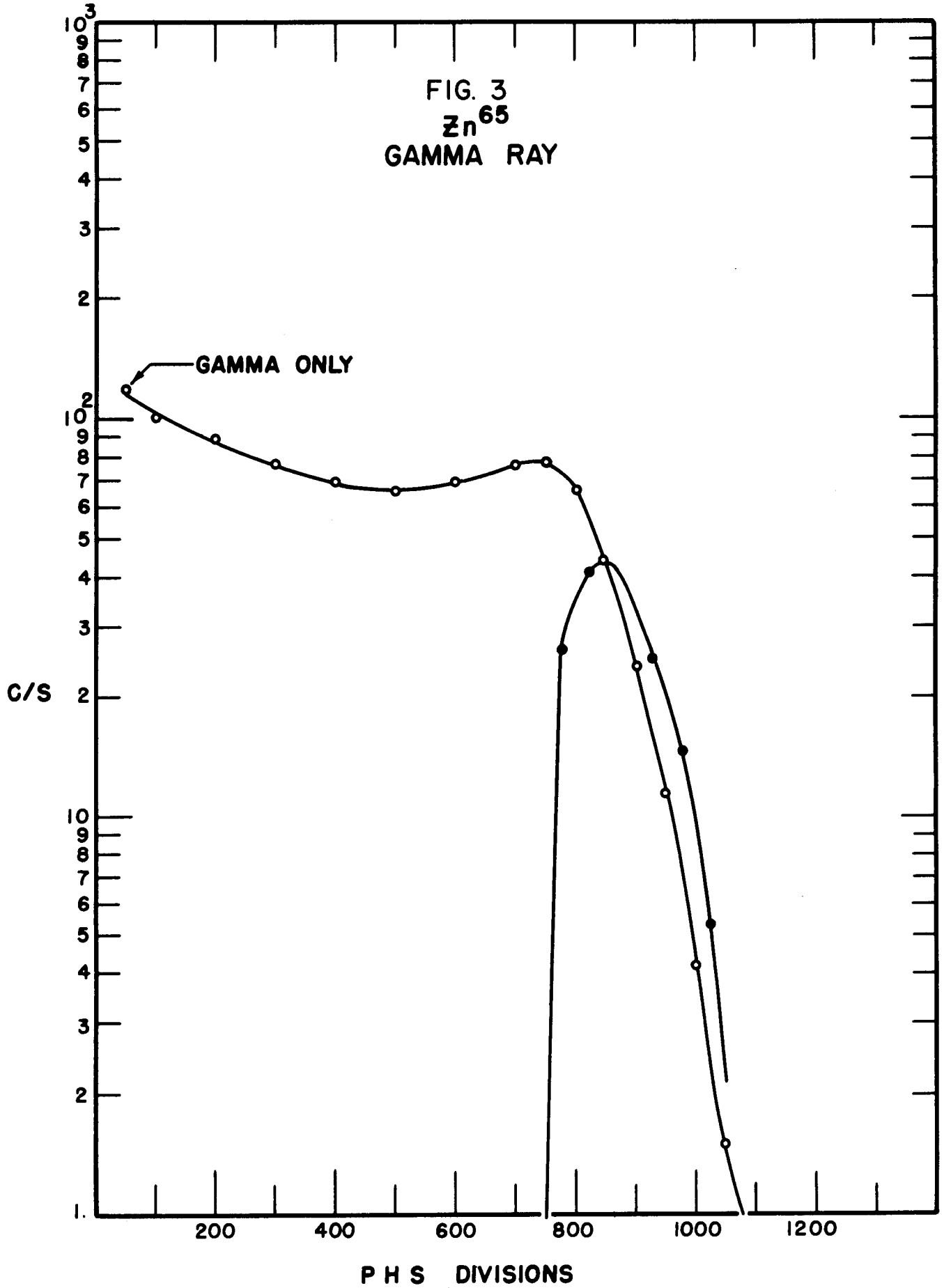
FIG. 3
Zn65
GAMMA RAY
GAMMA ONLY
C/S
PHS DIVISIONS
200
400
600
800
1000
1200

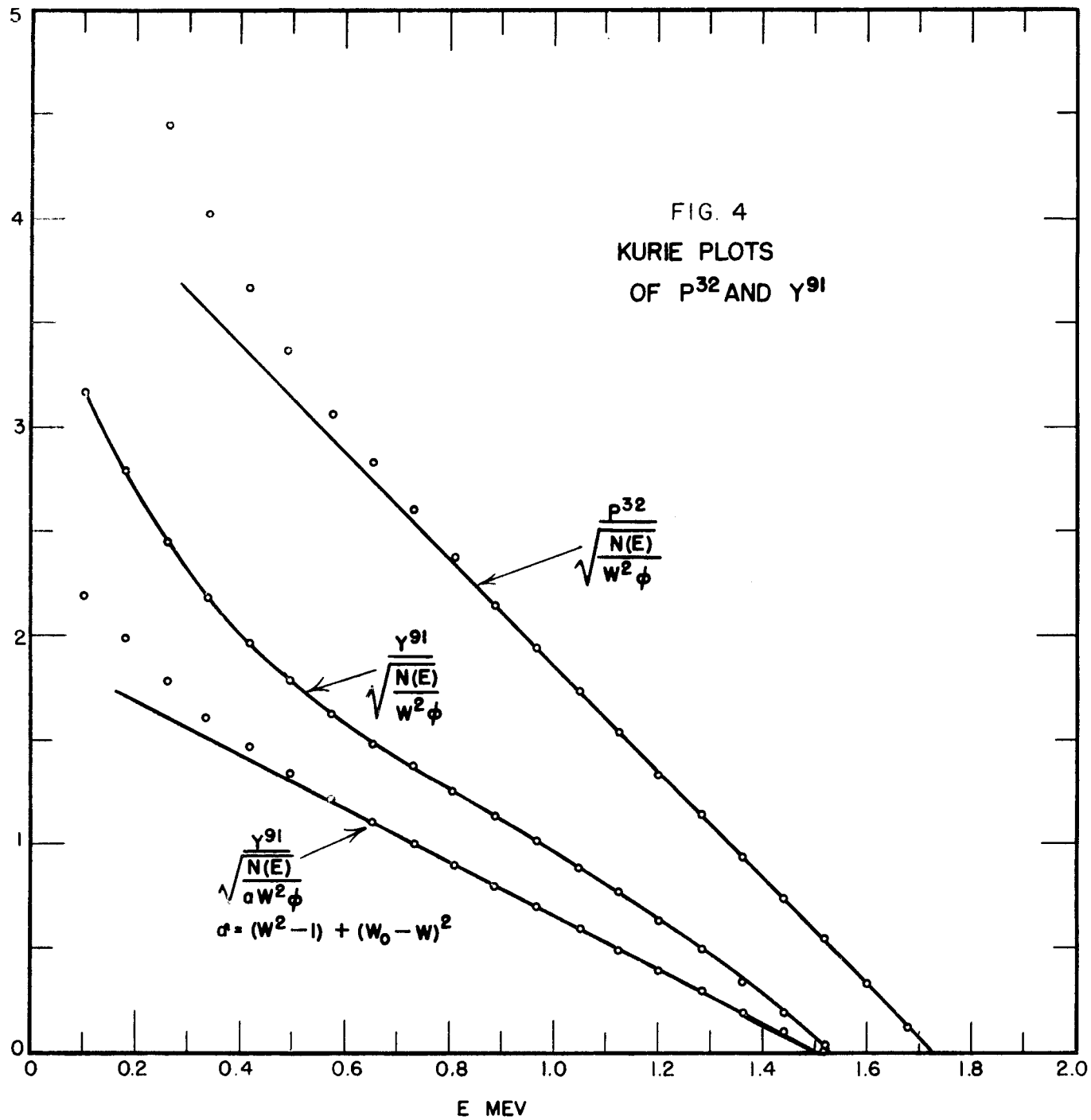
FIG. 4
KURIE PLOTS
OF P^{32} AND Y^{91}
$\sqrt{\frac{N(E)}{W^2\phi}}$ P^{32}
$\sqrt{\frac{N(E)}{W^2\phi}}$ Y^{91}
$\sqrt{\frac{N(E)}{aW^2\phi}}$ Y^{91}
$a = (W^2-1) + (W_0-W)^2$
0
1
2
3
4
5
0
0.2
0.4
0.6
0.8
1.0
1.2
1.4
1.6
1.8
2.0
E MEV

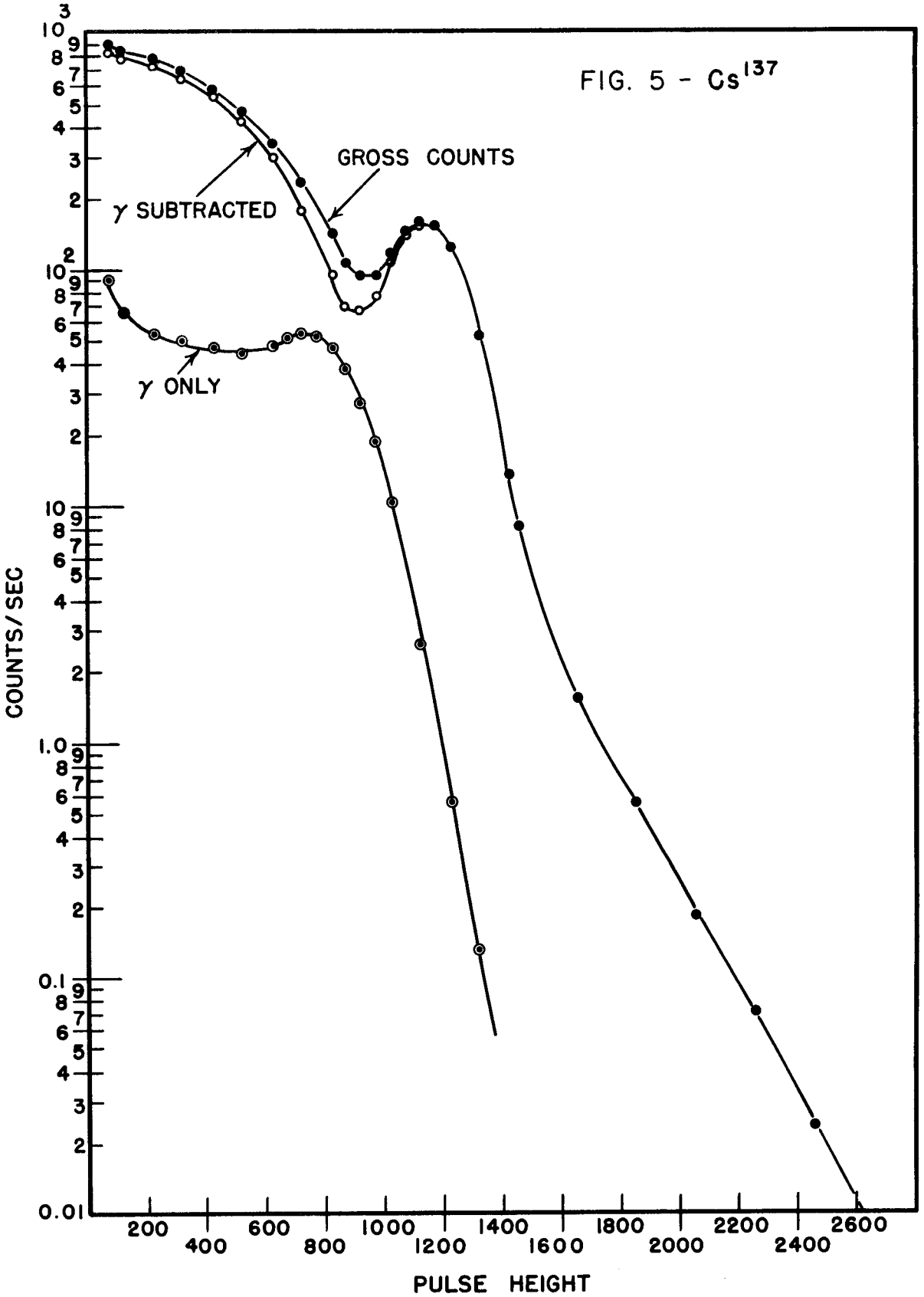
FIG. 5 - Cs137
GROSS COUNTS
γ SUBTRACTED
γ ONLY
COUNTS/SEC
PULSE HEIGHT
0.01
0.1
1.0
10
2
3
200
400
600
800
1000
1200
1400
1600
1800
2000
2200
2400
2600

estimating the contribution due to the upper β-ray. The normal Kurie plot is shown in Fig. 6. Also, the 1st forbidden correction, $p^2 + q^2$, was used and the straighter lower curve was obtained; the endpoint seems to be about 0.50 Mev. This beta-ray was found to have 1st forbidden shape during the course of the Be^{10} experiment.

A sample of BeO, chemically separated in 1944 by Levinger and Meiners from a beryllium target from the Washington University cyclotron, was used as source material. Six milligrams of the oxide were spread out about 2 mg/cm^2 thick on a 0.0002 in. thick polyethylene foil and counted in about 50% geometry. The specific activity was found to be about 18 disintegrations per second per milligram of Be in good agreement with the 17 ± 1 d/s per mg of Be found by Levinger and Meiners.

The plot of pulse height-number is shown in Fig. 7, both for the source and background. The background was not subtracted from the source curve. The feet on the points represent the standard deviation of the counting. The counter was shielded by 2 in. of lead for these runs to make the background small. The integral counting rate for the background was 1 c/s for all pulses larger than the size produced by a 25 kev electron.

Figure 8 shows the results on a linear plot (solid dots) with background subtracted. The open circle points are obtained by applying the Primakoff-Owen correction. The energy calibration was obtained by using the 630 kev electron peak from the data for Fig. 5. The correction is about the size of the standard deviation below 459 kev.

The beta spectrum of Be^{10} is of considerable interest because theory predicts an unusual shape for the spectrum. Kurie plots obtained from the data of Fig. 8 are shown in Fig. 9. The upper curve is the ordinary Kurie plot and it is obviously curved in the same sense as the plots for Y^{91} and Cs^{137}. The middle curve was obtained by using the factor $p^2 + q^2$, although this would not be expected to give a straight line since the spin change for the Be^{10}-B^{10} transition most probably has a spin change of three units. The lower curve is the result obtained when the theoretically expected correction factor, $p^4 + \frac{10}{3} p^2 q^2 + q^4$, was used. The fit for both of the corrected points to a straight line is about equally good although there does seem to be a slightly better fit for the $p^2 + q^2$ factor.

Both the normal Kurie plot and the $p^2 + q^2$ factor give an endpoint of 560 ± 10 kev, while the 2nd forbidden factor gives an endpoint of approximately 530 kev. The disagreement of any of these endpoints with the aluminum absorption

NOT CLASSIFIED
DWG. 7352

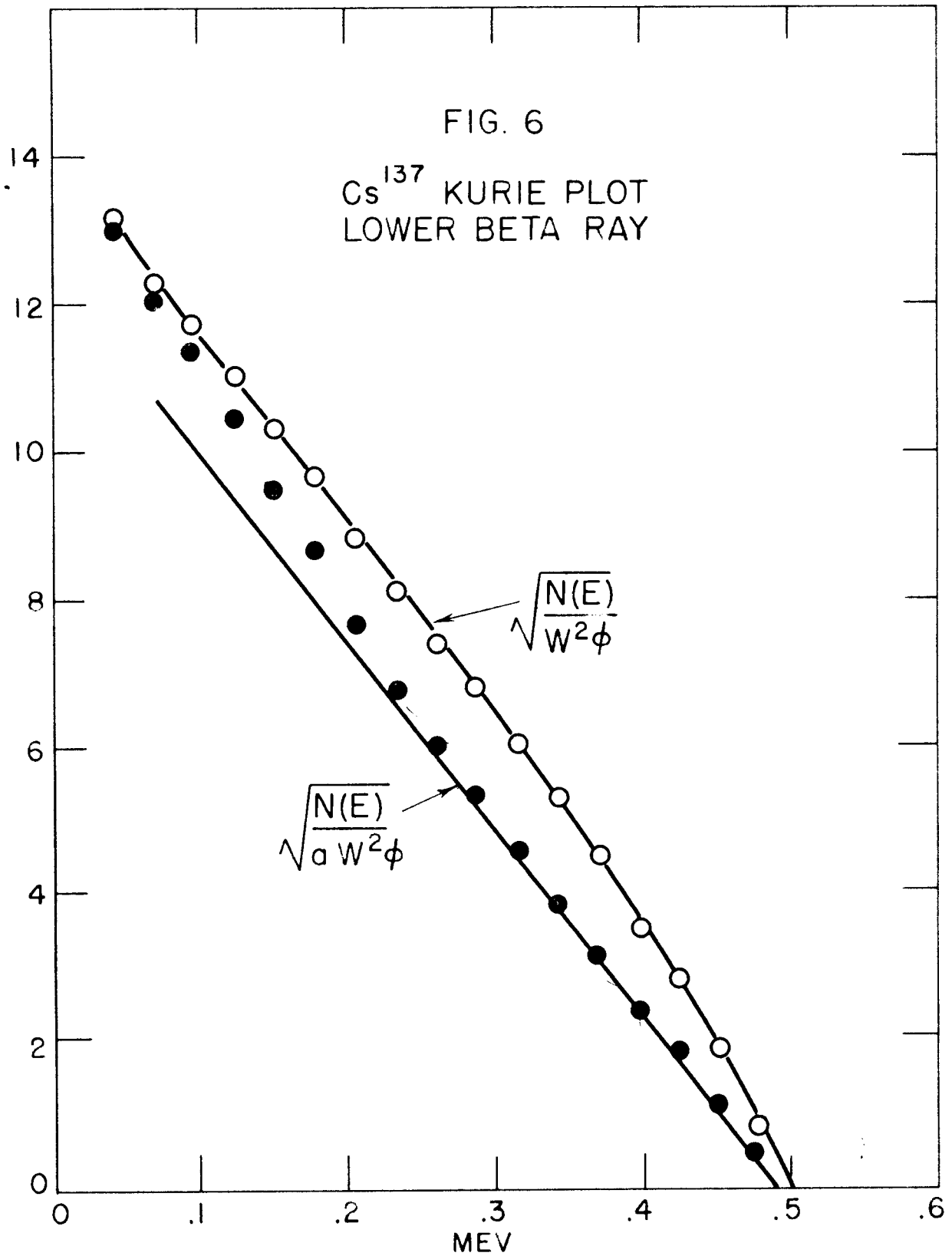

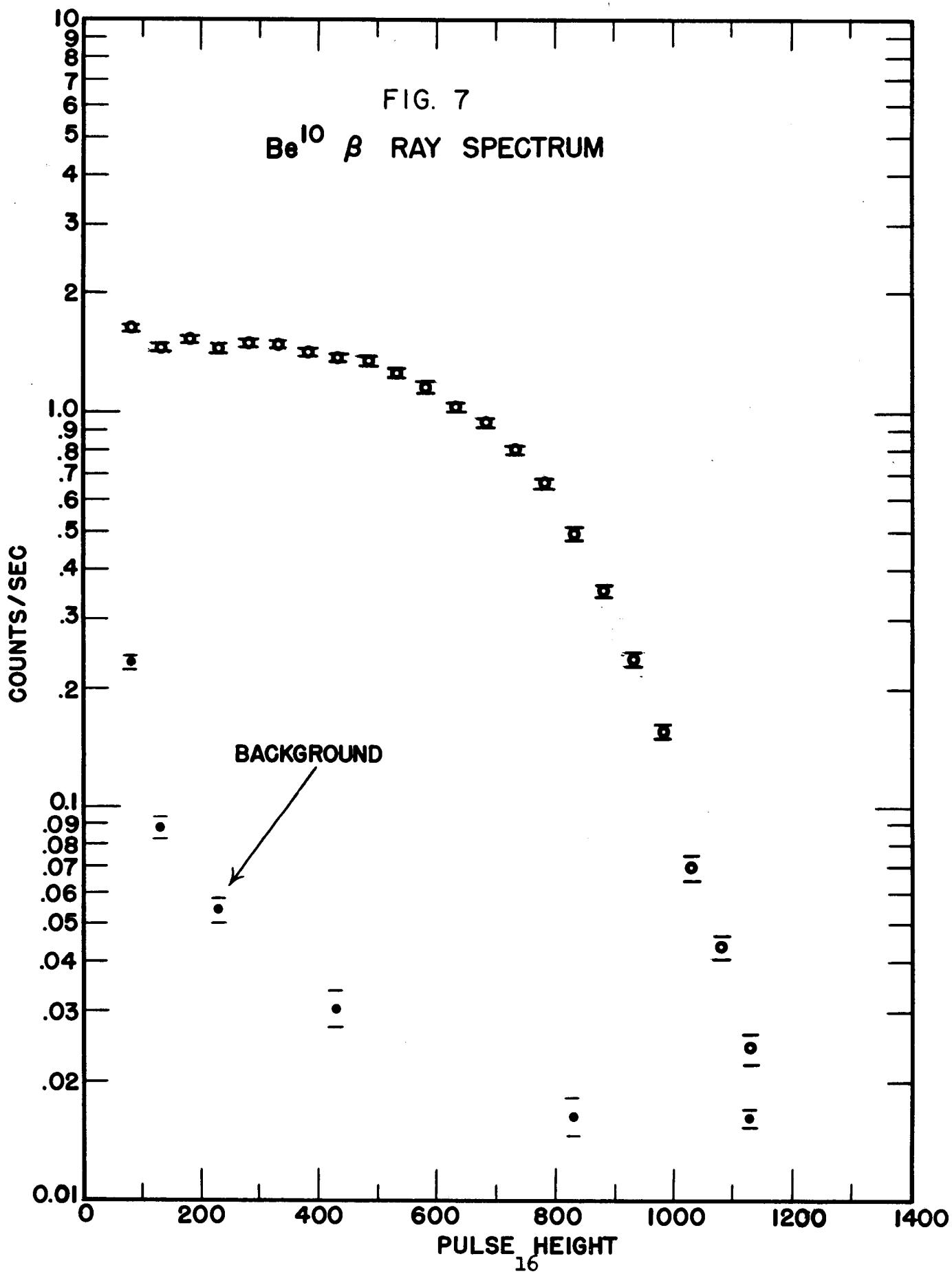
FIG. 7
Be10 β RAY SPECTRUM
COUNTS/SEC
PULSE HEIGHT
BACKGROUND
10
9
8
7
6
5
4
3
2
1.0
.9
.8
.7
.6
.5
.4
.3
.2
0.1
.09
.08
.07
.06
.05
.04
.03
.02
0.01
0
200
400
600
800
1000
1200
1400

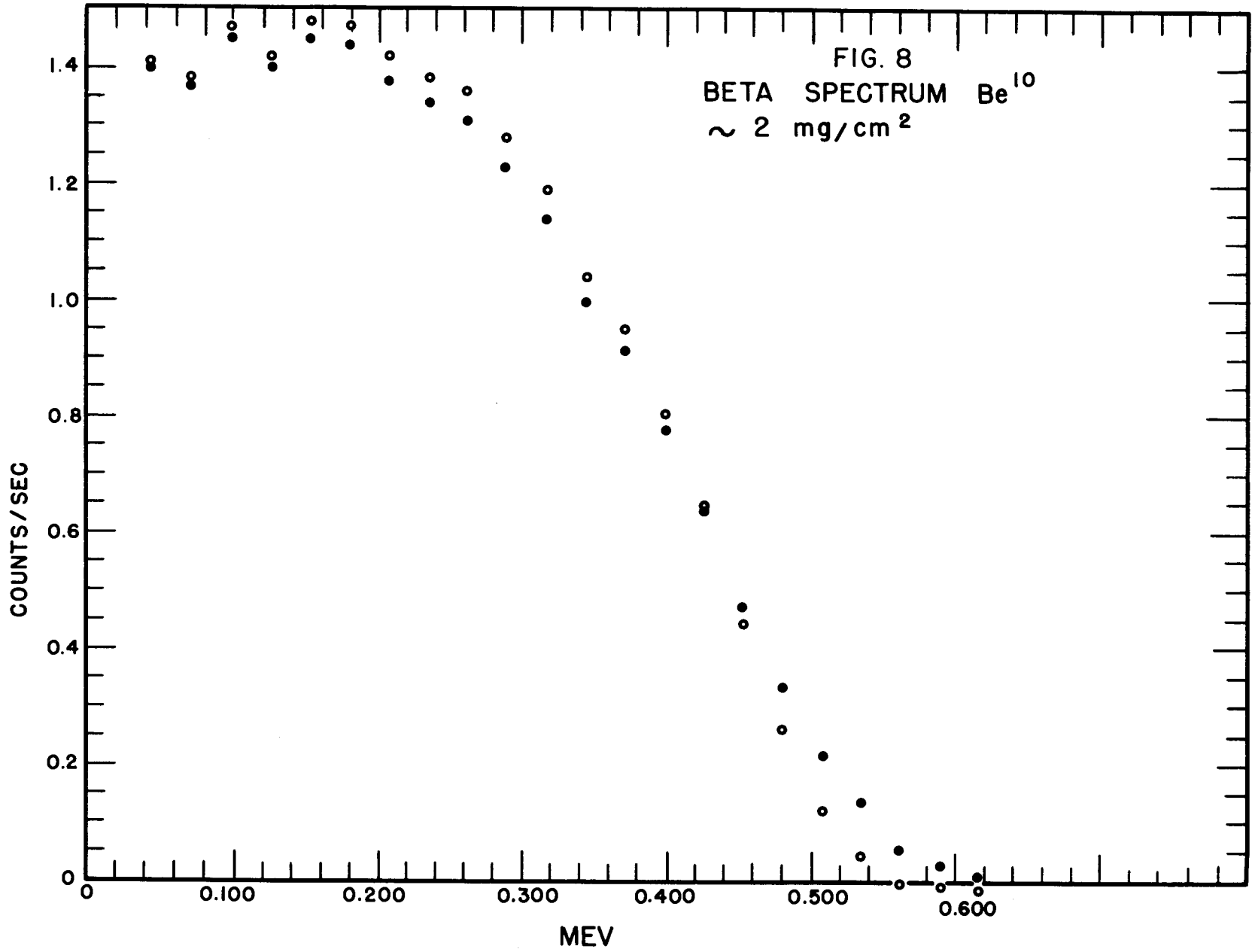
FIG. 8
BETA SPECTRUM Be10
~ 2 mg/cm2
COUNTS/SEC
1.4
1.2
1.0
0.8
0.6
0.4
0.2
0
0.100
0.200
0.300
0.400
0.500
0.600
MEV

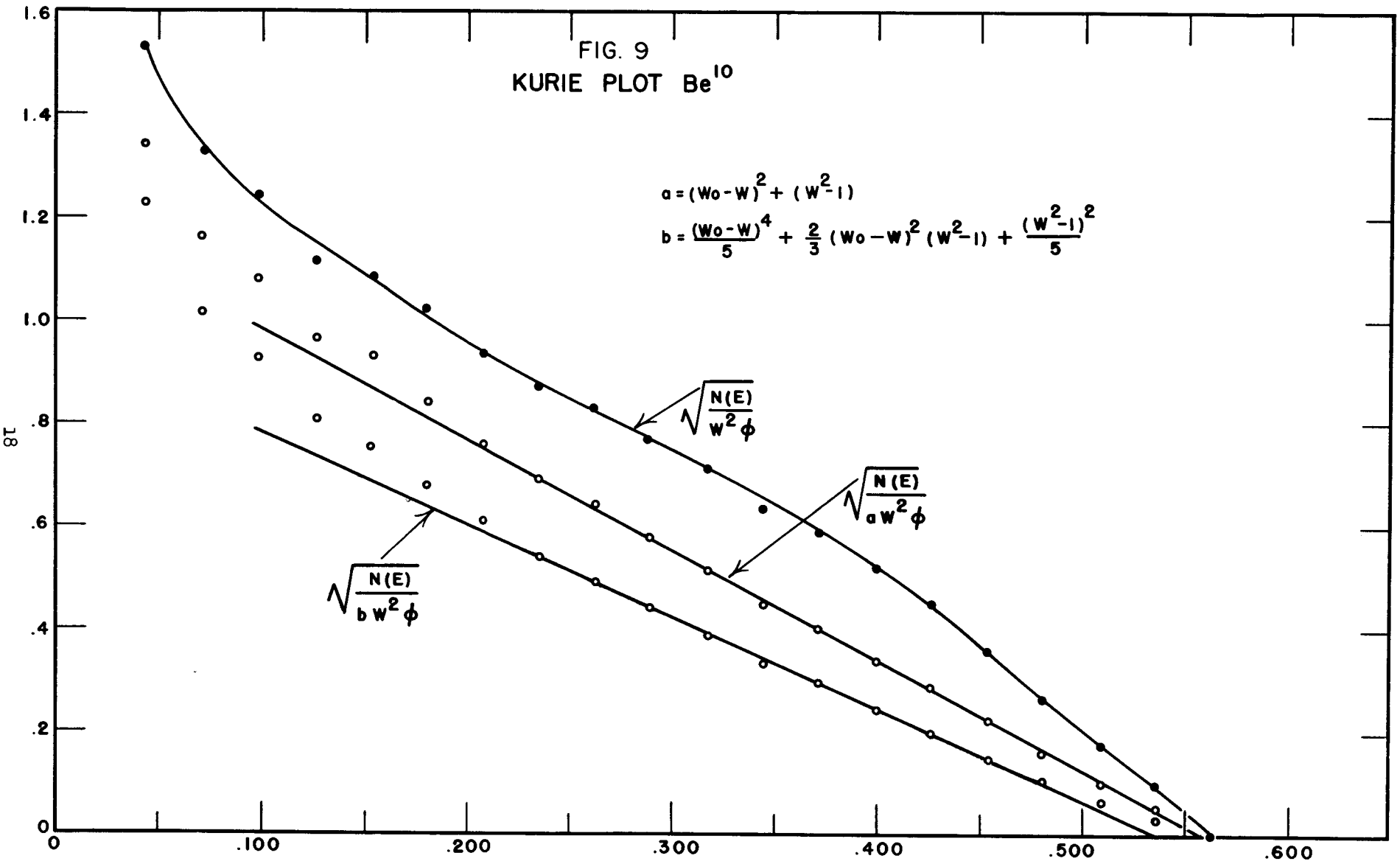
FIG. 9
KURIE PLOT Be^{10}
$a = (W_o - W)^2 + (W^2 - 1)$
$b = \frac{(W_o - W)^4}{5} + \frac{2}{3}(W_o - W)^2 (W^2 - 1) + \frac{(W^2 - 1)^2}{5}$
$\sqrt{\frac{N(E)}{W^2 \phi}}$
$\sqrt{\frac{N(E)}{a W^2 \phi}}$
$\sqrt{\frac{N(E)}{b W^2 \phi}}$
1.6
1.4
1.2
1.0
.8
.6
.4
.2
0
0
.100
.200
.300
.400
.500
.600

data of Hughes[3] is not surprising since, he attempted to avoid under-estimating the absorption endpoint by plotting the fourth root of the counting rate against absorber thickness and extrapolating to zero counting rate. The more rapid fall of counting rate with energy of electrons caused by the forbidden shape of spectrum would cause the extrapolated absorption data to give an endpoint of too high energy.

In order to apply the Primakoff-Owen correction to the scintillation counter data it is desirable to know the shape of output pulse distribution for a monoenergetic electron line at a number of energies. The Cs^{137} line served satisfactorily for the Be^{10} case since it lies close to the endpoint of the spectrum where the correction is important.

In order to extend this kind of correction, other conversion lines were measured. The metastable state of In^{115} appeared to be particularly attractive due to its convenient half-life (4.5 hours) and its easy production.

A sample was prepared by bombarding Cd metal foil for 18 hours in the pile; the sample was allowed to decay 24 hours to remove the 2.7 hr Cd activity leaving the 2.5 day and 43 day activities. The indium fraction was separated with indium carrier by sulfide precipitation of Cd in 0.3 *M* HCl. The Cd was allowed to stand some hours to allow the 4.5 hr indium to grow in from its 2.5 d parent, and the separation repeated. The indium was precipitated with a few mg of indium carrier as sulfide in .05 *M* HCl after removing the cadmium. The indium sulfide precipitate was dissolved in HNO_3 and the indium reprecipitated as hydroxide with excess NH_4OH. The precipitated indium was mounted on 0.0002 in. polyethylene and counted. The half-life was found to be 4.5 hrs and no activity was found after some days decay showing absence of the cadmium activities. The curves obtained on the scintillation spectrometer are those marked with triangles and open circles in Fig. 10.

It can be seen that the conversion line rests on a wide base of pulses. The whole curve decays with the same half-life. The curve with the open circles shows the expected single gamma ray. The broad part of the curve seems to be due to a beta ray with about 0.8 Mev maximum energy. The beta rays are about 0.2 times as numerous as the conversion line electrons. To make quite certain that the electrons of higher and lower energy than the conversion peak are real and not due to some defect of the equipment, a sample about 1000 times as strong was prepared and was run by B. Ketelle of the Chemistry Division, using the magnetic lens spectrometer. The curve shown by the solid dots in Fig. 10

[3] D. J. Hughes, C. Eggler, C. M. Huddleston, *Phys. Rev.* *75*, 515 (1949)

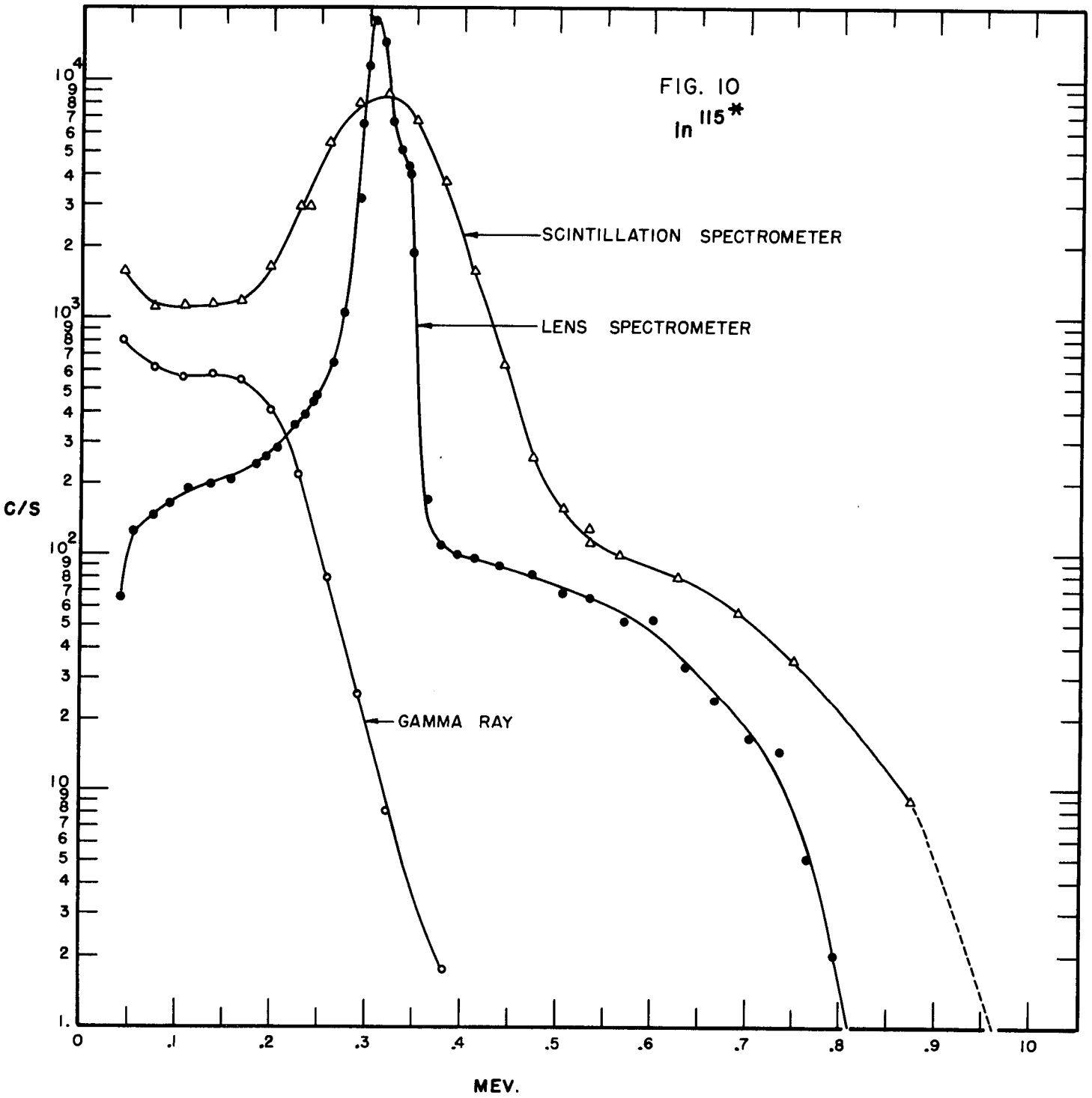
FIG. 10
In 115*
SCINTILLATION SPECTROMETER
LENS SPECTROMETER
GAMMA RAY
C/S
MEV.
10^4
10^3
10^2
10
1.
0
.1
.2
.3
.4
.5
.6
.7
.8
.9
10

was obtained. The same weak group of beta rays can be seen. Since the kind of defects to be expected in the two instruments are quite different, it seems likely that this beta ray group is real. The ratio of beta rays to conversion electrons found for the lens spectrometer was 0.12 and the Kurie plot made from Ketelle's data for the upper branch of the spectrum above the conversion line is shown in Fig. 11. The endpoint is about 830 kev. If the beta disintegrations go to the ground state of Sn^{115}, then the energy difference between In^{115} ground state and Sn^{115} ground state is the difference between the beta ray energy, 830 kev, and the isomeric transition gamma ray energy 340 kev. This makes the In^{115} unstable by 490 kev against beta disintegration.

An estimate of the fraction of the 340 kev gamma rays converted was obtained by measuring the beta ray spectrum of the 2.5 day cadmium freshly separated from the 4.5 hr indium daughter. Figure 12 shows, as curve A, the spectrum obtained. The next day the spectrum was re-run and shown as curve B. The 4.5 hr indium is practically in secular equilibrium with its parent. After 18 days the sample gave curve C, the remaining activity being mostly that of the 43 day cadmium, although the peak due to the conversion line is still visible.

Subtracting the 43 day activity from the two upper curves, correcting for the decay of the 2.5 day activity and subtracting permits the number of conversion electrons and the number of 2.5 day cadmium beta rays to be obtained. If all the 2.5 day cadmium decays go to the 4.5 hr indium, the indium gamma ray is about 25% converted. The gamma ray curves have been left off of the figure to make it clearer. This conversion percentage agrees moderately well with Lawson and Cork's estimate of 50%.

When a complete calibration of the gamma ray efficiency with energy is finished, the conversion coefficient can be measured directly by counting both electrons and the gamma rays. Estimating the gamma ray efficiency of the crystal from the Compton cross section, energy curves and the efficiency at 0.67 Mev, the percentage of the gamma ray corrected measures about 57%.

The maximum energy of the beta rays from the 43 day cadmium was also estimated to be about 1.8 to 1.9 Mev.

It has been found that a weak magnetic field has a serious effect upon the pulse size produced by the C-7132 photomultiplier tube. The earth's field is large enough to cause a two to one change in pulse size if directed through the tube in the most favorable and unfavorable way. It has been found by Max Goodrich, Physics Division, that a field of from a .1 to 0.5 gauss directed along the axis of the 1P21 part of the dynode structure in the tube, in such a

NOT CLASSIFIED
DWG. 7353

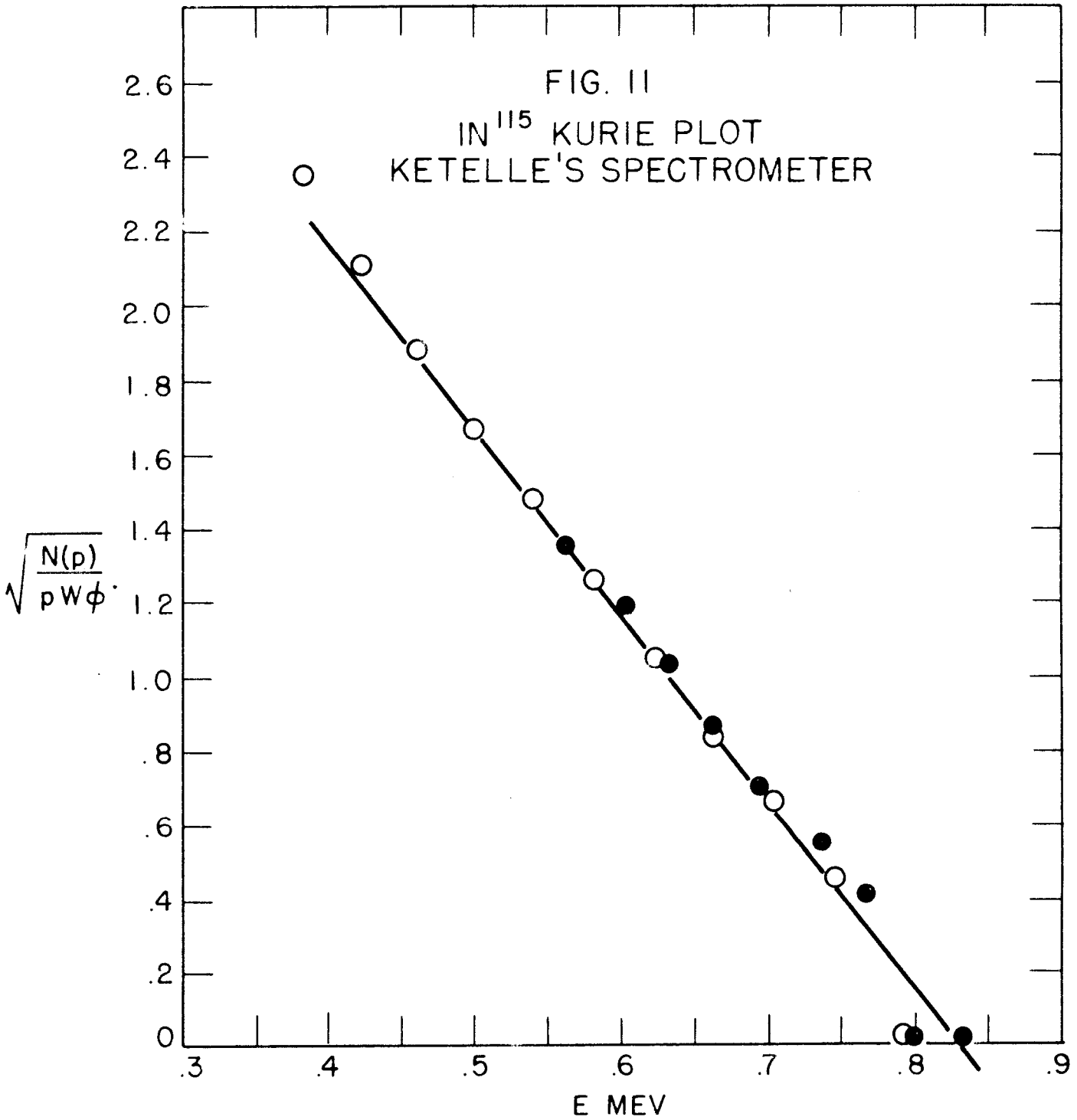

UNCLASSIFIED
DWG. 7410

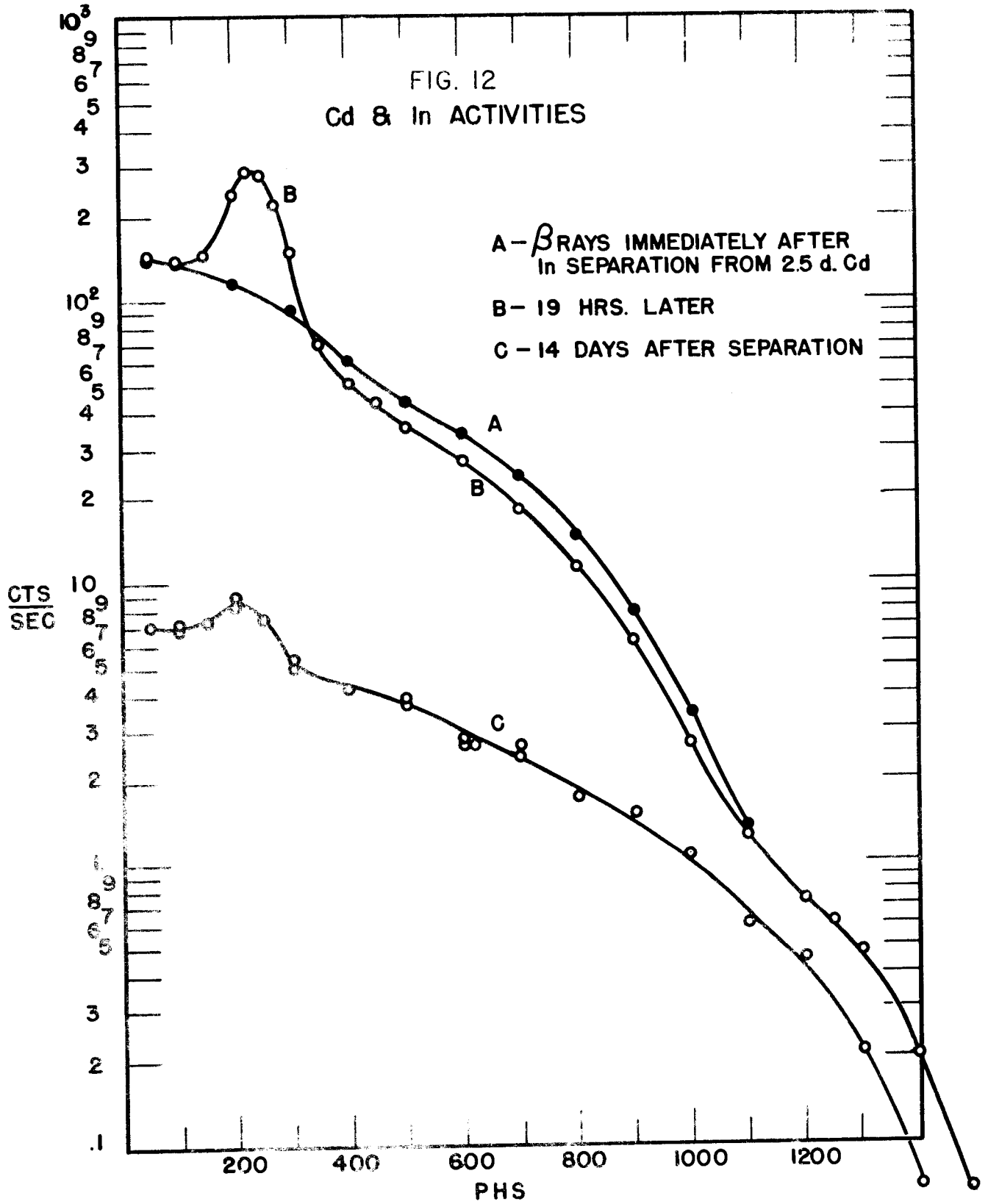

sense as to bend photoelectrons emitted from the first dynode toward the second dynode, produces considerable improvement. This effect does not appear to be present in the 1P28 or 1P21 photomultiplier tubes.

A considerable improvement is also found if the voltage between the photocathode and the first dynode is raised from 50 volts to about 200 volts. The resolution obtainable with the best anthracene and the best present arrangements of the phototube is illustrated by Fig. 13. This is the spectrum of Cs^{137} and the improvement in resolution can be seen by comparing with the similar curve shown in ORNL 228.

Work is now in progress on a two tube, two crystal equipment for coincidence work or for counting all beta rays leaving a sample.

High Speed Oscilloscope (George Kelley). Since the last report a preamplifier has been added to this oscilloscope. The unit was designed to have a considerably greater pass band than the deflection amplifier in order to preserve essentially the same speed of response.

The circuit is given in Fig. 14. It consists of two, three-tube distributed stages each having a gain of about 5, joined through a coupling tube. An eighth tube is used to couple this second stage to the delay line input and to the synchronizing circuit input. Figure 15 shows the construction of the coils for both the preamplifier and the deflection amplifier. Rise time of the unit probably is between 3×10^{-9}, and 4×10^{-9}, and the gain is about 25. Input is through a 200 ohm ladder attenuator having a maximum attenuation of 20 db obtained in steps of 4 db. This input may be fed directly from the apparatus under test in cases where this 200 ohm lead is not objectionable. For other purposes a probe is being constructed to provide a low admittance input.

The preamplifier is connected to the deflection amplifier through 133 feet of Amphenol 72-30 cable having a characteristic impedance of 195 ohms, which gives a delay of 1.5×10^{-7} seconds. Rise time of the entire system from attenuator to deflection plates is between 5×10^{-9} and 6×10^{-9} sec, and the overall gain is of the order of 10^3. A picture of the oscilloscope and its power supplies is given in Fig. 16.

Several changes have been made in the deflection amplifier. The plate and grid line impedances were reduced to 450 ohm and 340 ohm, respectively, and its design improved, making the inductance values given in the last report incorrect. A small inductance (0.5 μH) is added in series with the input from the delay line to provide a better termination for this line. A new type cathode ray tube, the 5XP-11 was installed. Due to its increased deflection

NOT CLASSIFIED
DWG. 7411

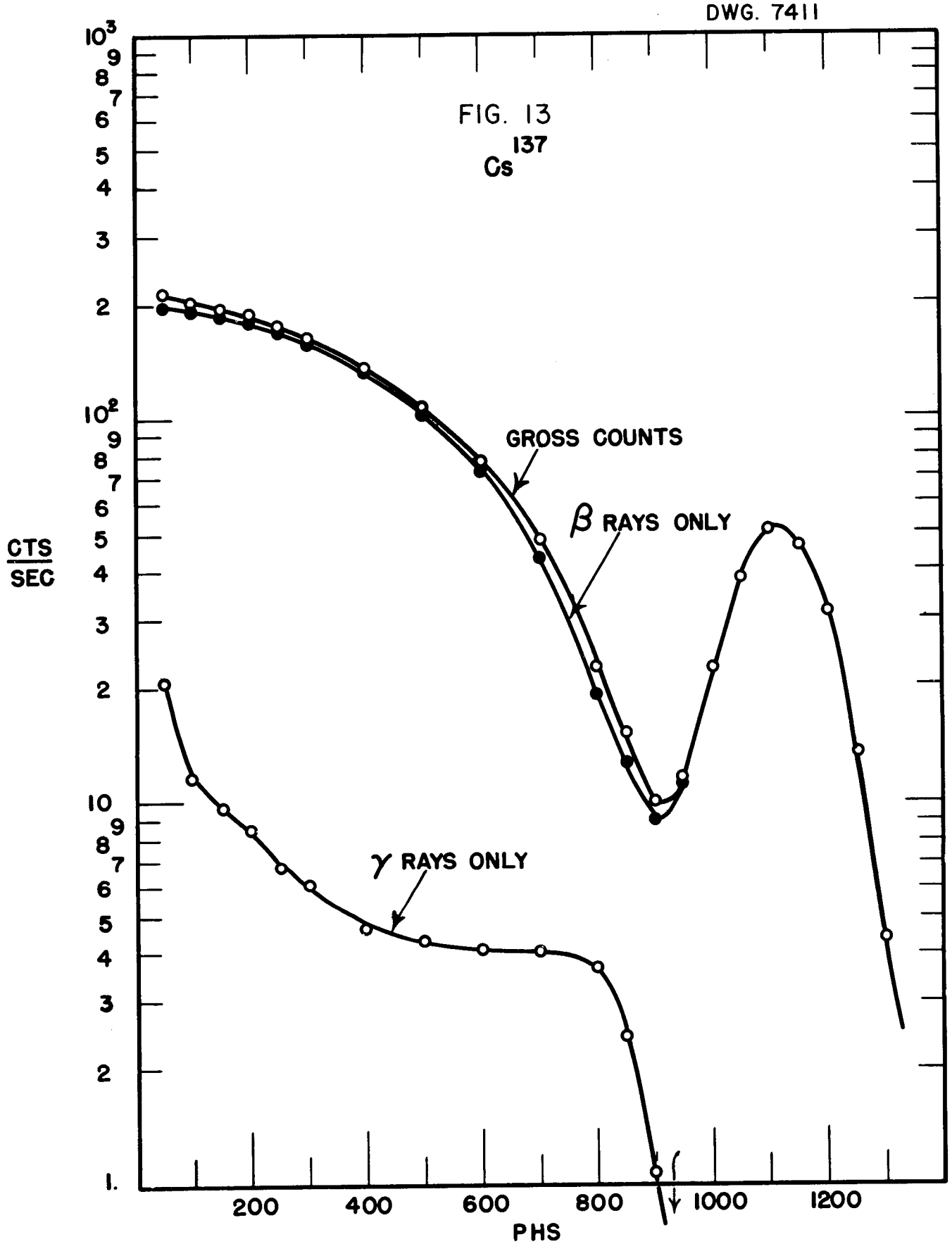

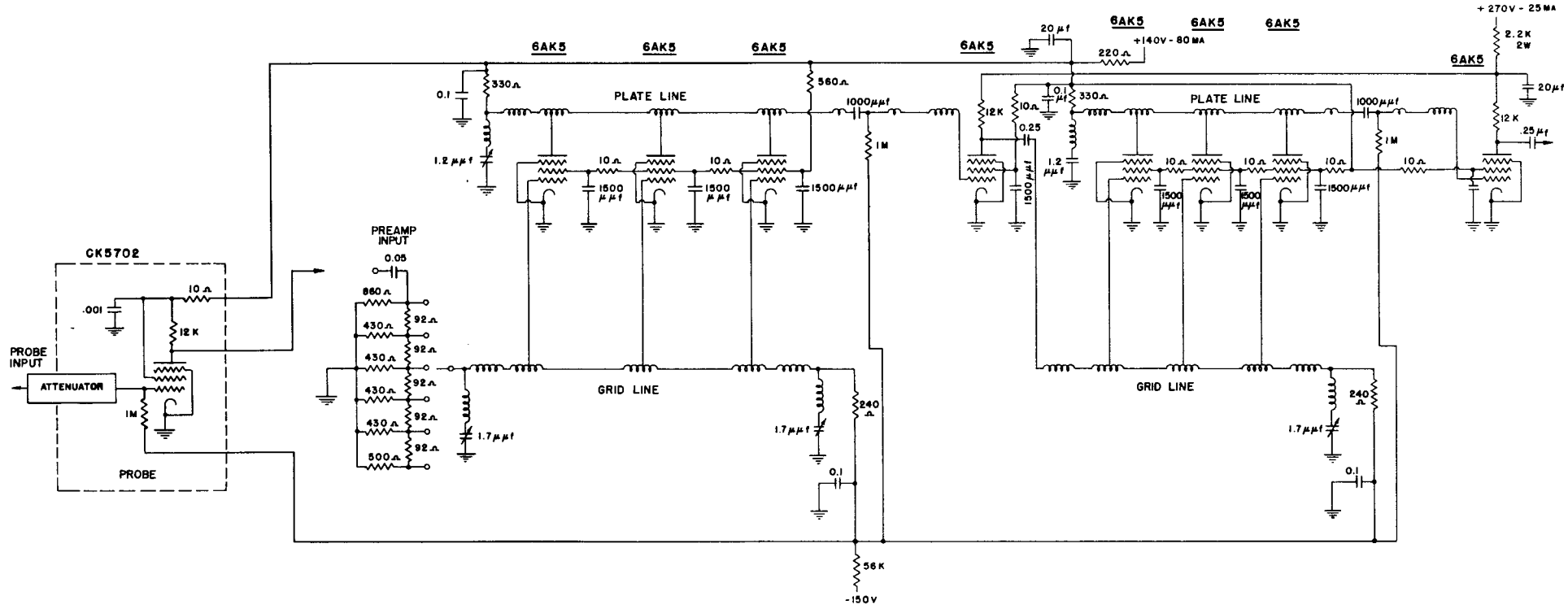

PREAMPLIFIER AND PROBE
FOR
MODEL S-1 SYNCHROSCOPE

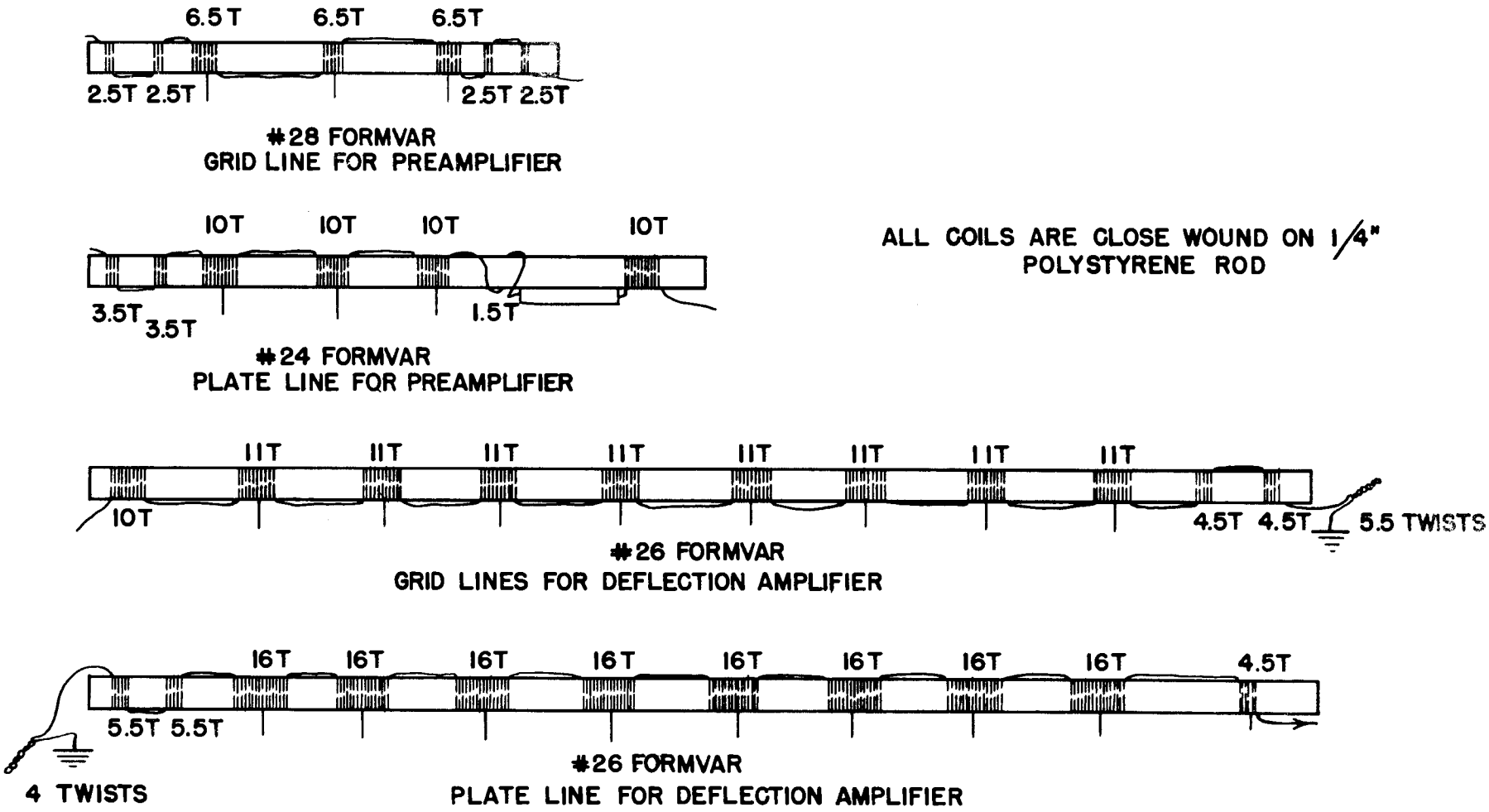

FIG. 15
COILS FOR S—1 SYNCHROSCOPE

NOT CLASSIFIED

Dr. 6936

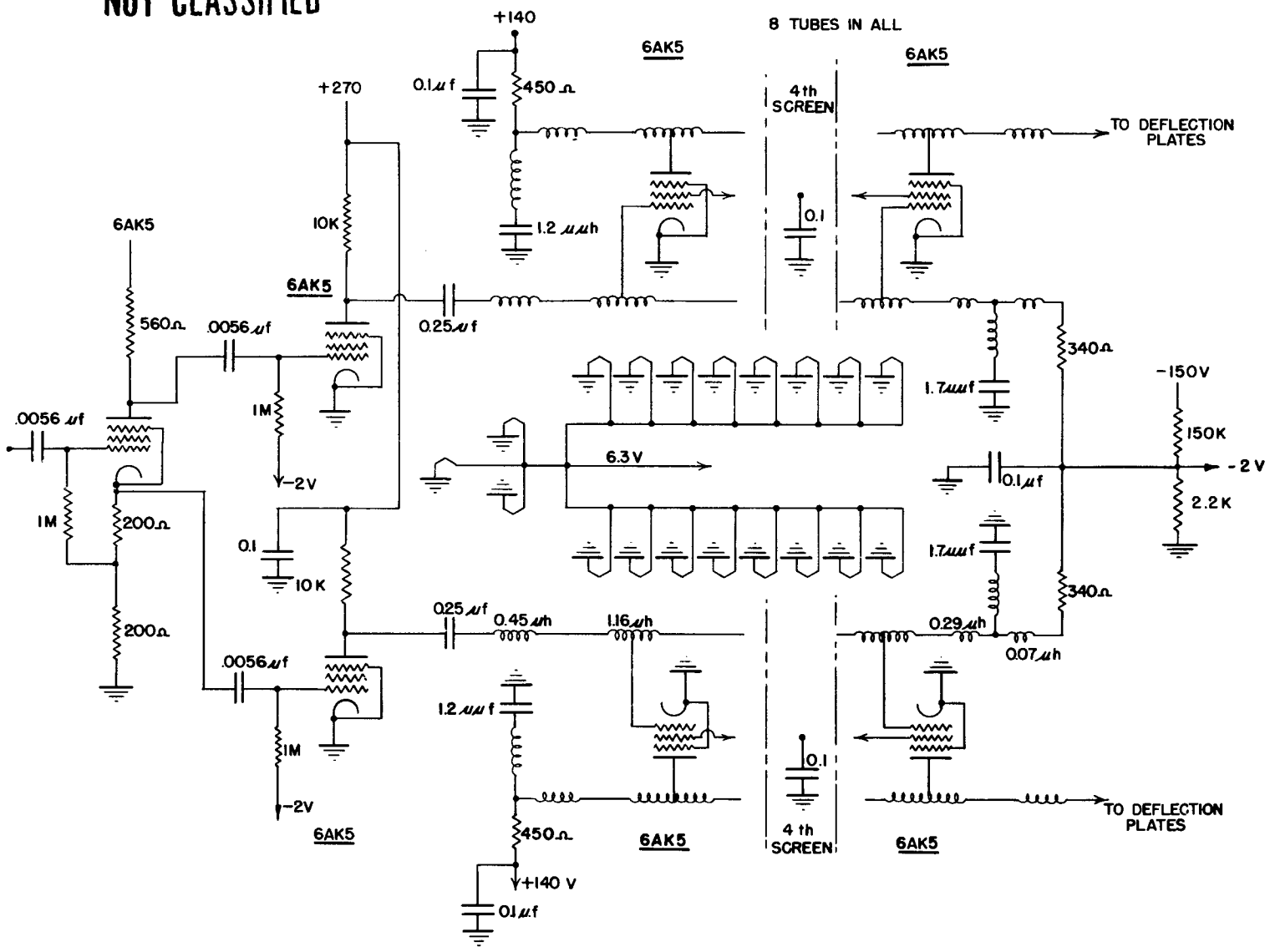

FIG. 16
DEFLECTION AMPLIFIER
FOR
MODEL S-I SYNCHROSCOPE

sensitivity, a usable deflection of nearly an inch in either direction may be obtained.

The high speed oscilloscope has been used to measure the decay constant of various phosphors. Figure 17 is illustrative of the data obtained. The photographs are of waveforms obtained from individual light pulses from the phosphor under excitation from caesium β-rays. In Fig. 17, photographs a, b, and c are obtained from Stilbene, Anthracene and Naphthalene, respectively. Photograph d was obtained by discharging a 100 $\mu\mu$f condenser into the 200 Ω input attenuator and serves as a check on these measurements. The following tabulation gives the results obtained at room temperature:

PHOSPHOR	*DECAY CONSTANT (μsec)*
Phenanthrene	0.0083 ± 20%
Stilbene	0.010 ± 20%
Anthracene	0.022 ± 10%
Fluorene	0.02 ± 20%
Fluoranthene	0.055 ± 10%
Naphthalene	0.070 ± 10%

All the decay curves appear to be exponential. There is some doubt about the calibration of the time scale so the values given may possibly be wrong by a constant factor.

Short-Lived Isomers (F. K. McGowan). **Instrumentation.** The method of delayed coincidences between two anthracene scintillation counters has been extended to measure time intervals in the region 10^{-8} sec or longer. The unit is considerably simplified over previous units used for measuring time intervals in the region 10^{-7} to 10^{-3} sec. The video amplifier, designed by Bell and Jordan, has a rise time of approximately 10^{-8} sec and a maximum gain 240. The two amplifier sections were constructed during the early fall of 1948 by J. E. Francis. It was originally planned to use two multiplier tubes in coincidence for each crystal, in order to reduce the thermionic noise. After some thought this scheme was abandoned for two reasons: (a) One needs signals of a few volts amplitude at the output of multiplier to operate a coincidence stage properly, and (b) there is a loss of solid angle for light collection subtended by the crystal to the two photo-cathodes. It seemed desirable then

NOT CLASSIFIED
DWG. 7412

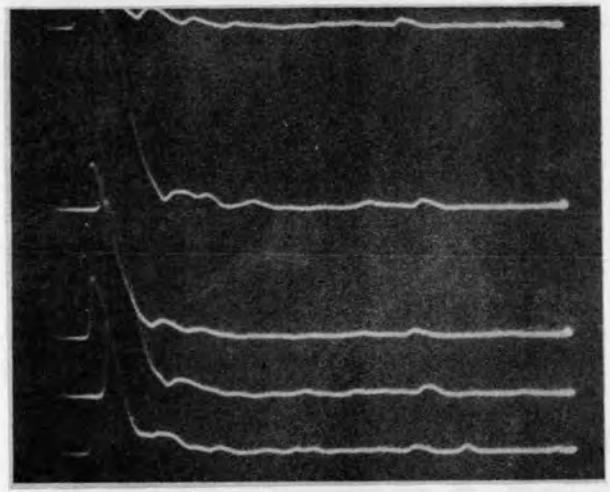

a- STILBENE

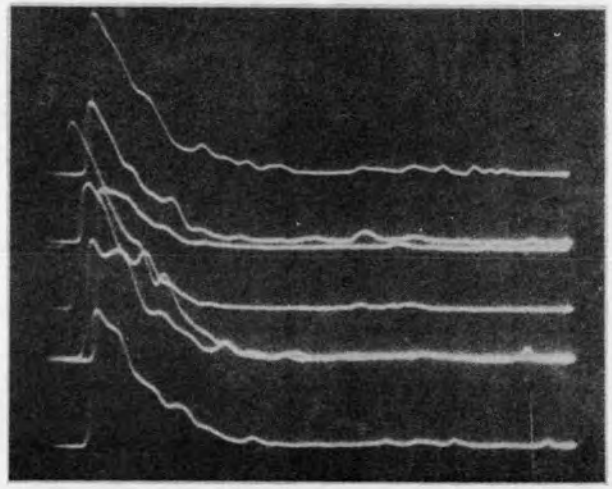

b- ANTHRACENE

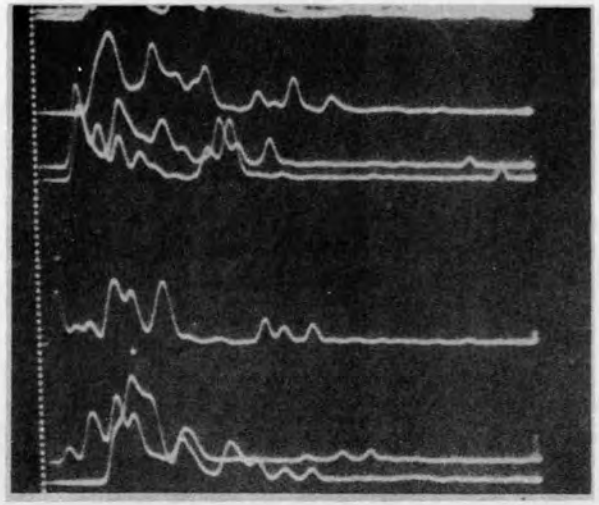

c- NAPTHALENE

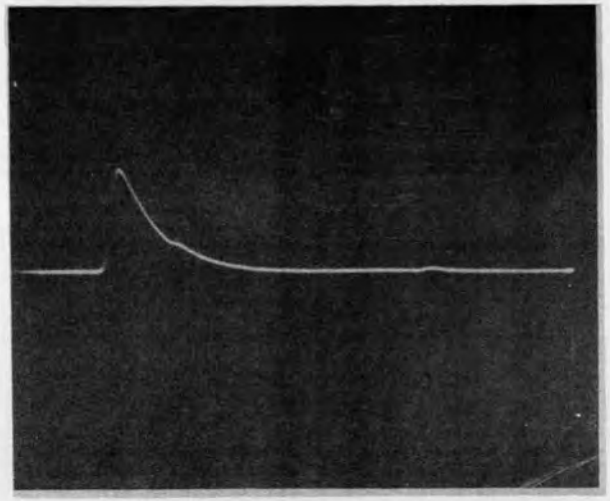

d- CALIBRATING PULSE OF 0.021μ SEC TIME CONSTANT

LIGHT PULSES FROM SCINTILLATION PHOSPHORS

to try operating the unit using two multipliers, each looking at a crystal, raising the voltage per stage slightly so that most of the pulses due to a scintillation saturated or nearly saturated the amplifier, and doing pulse height selection at the input of the scaler. A complete circuit diagram including video amplifier, pulse forming, coincidence stage, and pulse lengthening is shown in Fig. 18.

The 1P21 tubes, selected for high gain, are operated at approximately 80 volts per stage and the tubes and crystals are cooled to dry-ice temperature. The background (single counts) with crystals in place is ~150 c/m of which only 10 c/m is due to thermionic electrons leaving the photo-cathode. This corresponds to a pulse discrimination level such that incident radiation as low as 75 kev energy (probably lower) is being detected. Figure 19 shows the number of coincidences as a function of delay time obtained with a β^- emitter, Tl (3.5 yr). The majority of the sources used give similar curves exhibiting a sharp break at 8×10^{-8} sec. The resolving time of the coincidence circuit is 4×10^{-8} sec and is kept constant. With the present arrangement of anthracene crystals and 1P21 tubes, the instrument is probably capable of measuring a reasonably intense isomeric state with a half-life $\geqslant 3 \times 10^{-8}$ sec. We expect some improvement when the 1P21 tubes are replaced by the C-7132 tubes and stilbene crystals are used.

Results Last quarter it was reported that 4 radioisotopes being investigated might be decaying to isomeric states with half-lives $< 10^{-7}$ sec. These cases were Hg^{203}(43 da) Tl^{203}, Ta^{182}(117 da) W^{182}, Ir^{192}(72 da) Pt^{192}, and Yb^{169}(33 da) Tm^{169}. With the faster unit there is no indication of any short-lived isomeric state, indicating that the excess counts obtained with the slower unit were instrumental. As an additional check, a source of Hg(43 da) was simulated using β^- rays of Ca^{45} and the internal conversion line of In^{114*}. The coincidences as function of the delay with the slower unit indicated a slight excess of counts above the expected random rate. This instrumental effect is due to a small signal in the channel for detecting the delayed radiation and a large simultaneous signal originating in the channel for announcing the formation of the isomeric state.

Using a sample of enriched Cd^{110} to form the reaction Cd^{110} (n,γ) Cd^{111**} $\xrightarrow[48\ \text{min}]{\gamma,\ e^-}$ Cd^{111**} $\xrightarrow[8 - 9 \times 10^{-8}\ \text{sec}]{\gamma,\ e^-}$ Cd^{111}, the existence of the short-lived

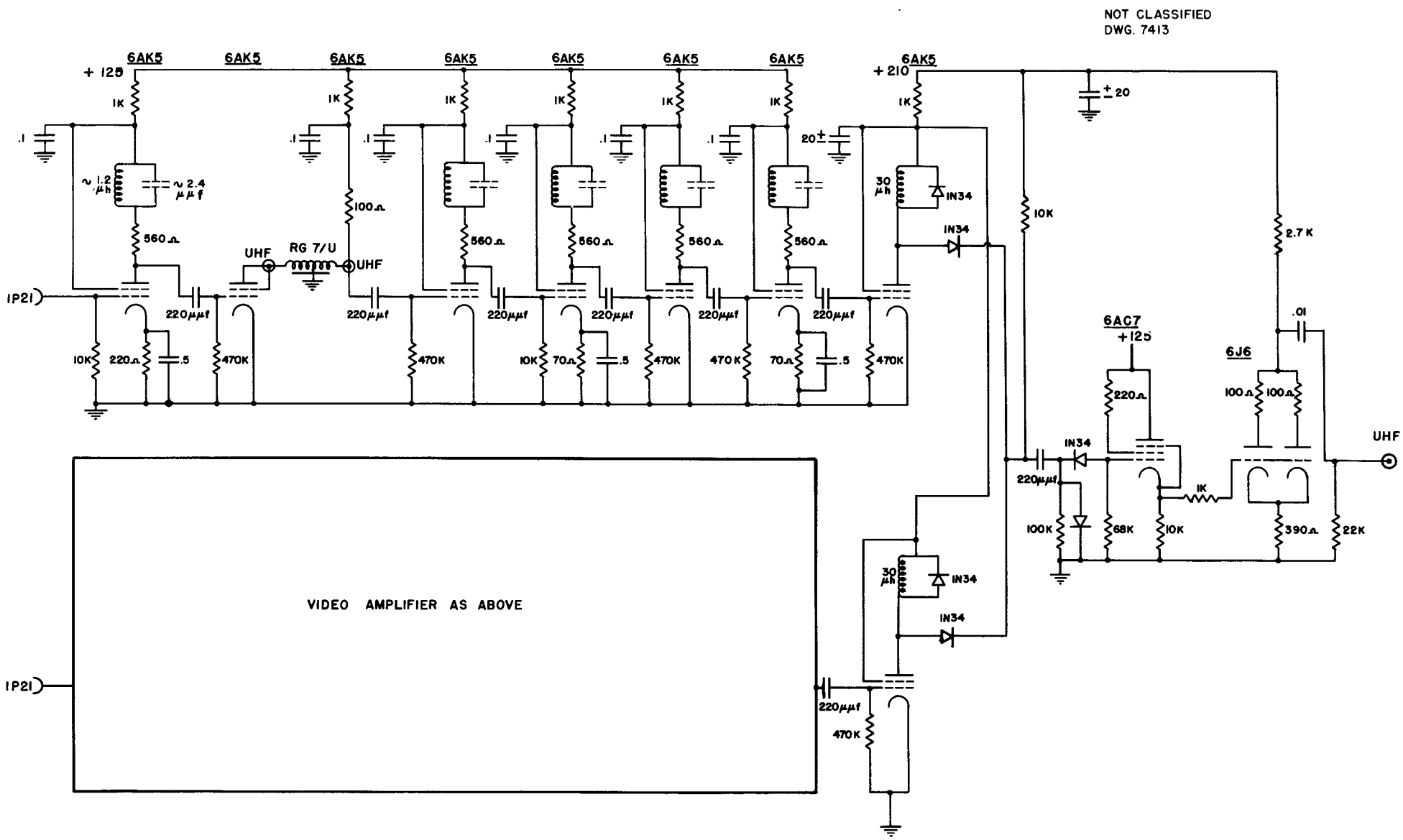
NOT CLASSIFIED
DWG. 7413
6AK5
+ 125
+ 210
1K
.1
~ 1.2 μh
~ 2.4 μμf
560Ω
100Ω
UHF
RG 7/U
1P21
220μμf
10K
220Ω
.5
470K
70Ω
20±
30 μh
IN34
10K
2.7K
± 20
.01
6AC7
+125
6J6
100Ω
68K
390Ω
22K
VIDEO AMPLIFIER AS ABOVE

FIGURE 18

UNCLASSIFIED
DWG. 7409

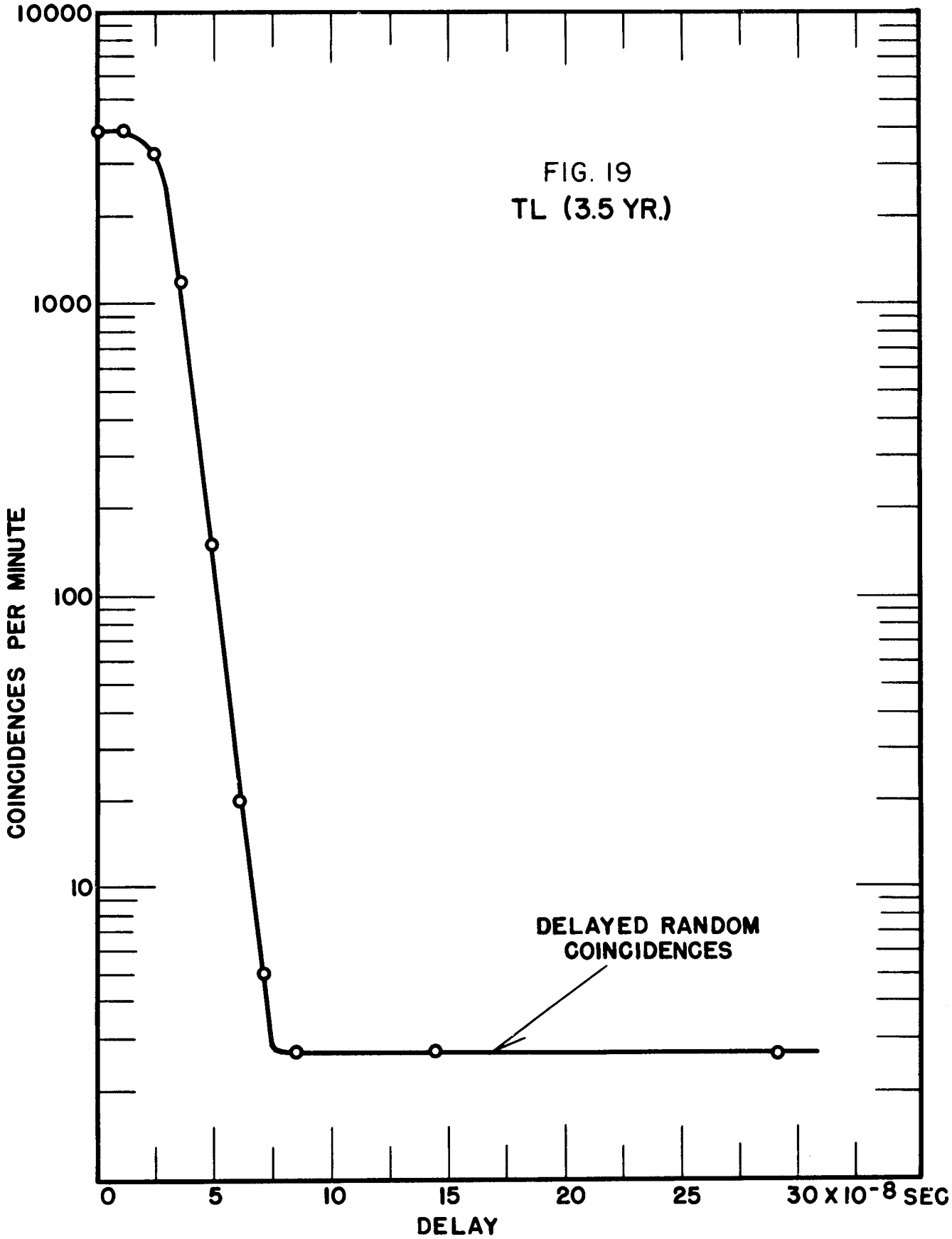

isomeric state of Cd^{111} previously reported by Deutsch (*Bull. Am. Phys. Soc.*, Washington Meeting 1949, p. 32) was confirmed. Deutsch originally reached the metastable state by K capture decay of In^{111} and later by Cd^{111*} (48 min). Figure 20 shows the delayed coincidence curve obtained with a source of Cd^{111}. The value of the half-life was found to be $(9 \pm 1) \times 10^{-8}$ sec. Using a source of $Ag^{111} \xrightarrow[7.5\ da]{\beta^-} Cd^{111}$, the number of coincidences as a function of delay time indicated that Ag^{111} decays directly to the ground state of Cd^{111}.

The following radioisotopes have been investigated for short-lived isomeric states in the region 3×10^{-8} sec to 10^{-3} sec:

Ag^{110}(225 da) Pd^{110}, W^{185}(73 da) Re^{185}, Yb^{169}(33 da) Tm^{169} (exclusive of the 1 μ-sec isomeric state), Cd^{115}(43 da) In^{115}, Ti^{51} (72 da) V^{51}, Hg^{203}(43 da) Tl^{203}, Ir^{192}(72 da) Pt^{192}, Ta^{182}(117 da) W^{182}, Se^{75}(115 da) As^{75}, Ag^{111}(7.5 da) Cd^{111}, Pd^{109}(13 hr) Ag^{109}, Sb^{124}(60 da) Te^{124}, Tm^{170}(125 da) Yb^{170}, Sm^{153}(46 hr) Eu^{153}, Dy^{165}(2.5 hr) Ho^{165}, Nd^{149}(1.7 hr) Pm^{149}, $Gd^{161?}$(18 hr)$Tb^{161?}$, Ho^{166}(27 hr) Er^{166}. Hf^{181}(46 da) Ta^{181} (exclusive of 22 μ-sec isomeric state). No delayed coincidences above the expected delayed random coincidence rate were detected.

The pure rare earths used in these experiments were produced by Dr. Boyd and D. H. Harris of the Chemistry Division.

NOT CLASSIFIED
DWG. 7356

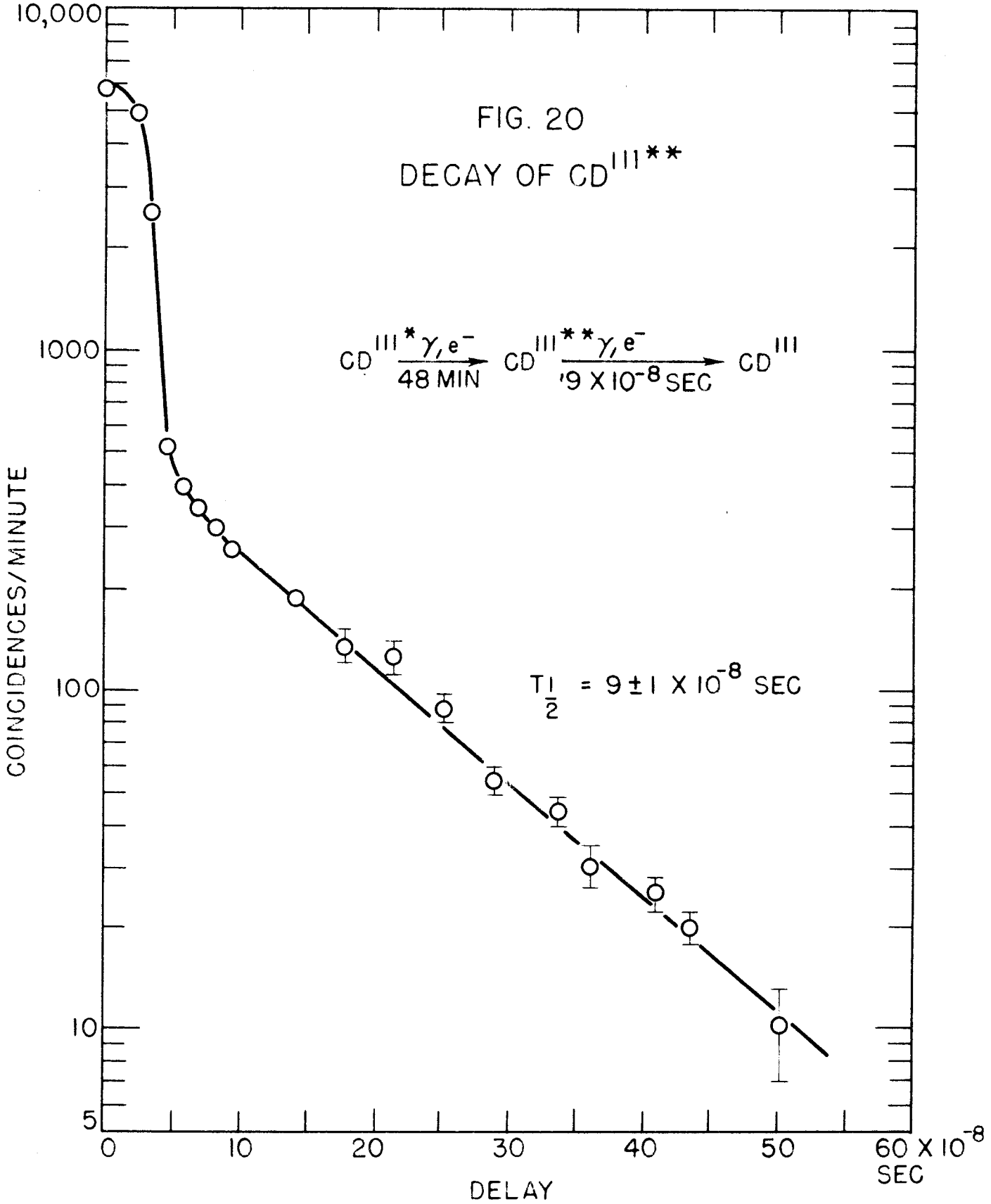

SEMI-CONDUCTORS

Semi-Conductor Research (Karl Lark-Horovitz, Jay Cee Pigg).* In continuation of the experiments by W E. Johnson, Dr. Lark-Horovitz, and Jay Cee Pigg, experiments were carried out to investigate (a) the characteristic of Germanium mixer crystals as a function of neutron bombardment, and (b) the behavior of high back voltage crystals, IN46's at room temperatures and IN38's at about 193° K. In addition, one N type germanium sample was bombarded to a total of 4.37×10^{18} integrated neutron flux, and a silicon sample sealed in a pyrex-envelope was bombarded to a total of 2.62×10^{18} integrated neutron flux.

The IN47 rectifier behaves essentially like all other high back voltage crystals; at low forward bias and in the back direction the conductance increases as a function of bombardment. At a forward bias above 0.2 volts the conductance first decreases and then increases indicating an appreciable influence of spreading resistance.

Following a suggestion of M. A. Bredig and R. P. Metcalf a simple cryostat was designed to be used in a vertical central hole (hole 12) so as to expose semi-conductors at a known low temperature. For this purpose, concentric cylindrical cans separated by strips of balsa wood were filled with butyl cellusolve and dry ice. To avoid fluctuations due to bubbling of the dry ice mixture, the crystal was held in a quartz tube filled with butyl cellusolve. The temperature was read by a thermocouple held in proximity to the crystal. At the present time, the behavior of the crystal is essentially similar to what has been observed at room temperature. Relaxation effects still exist since upon shutting off the pile the resistance has a tendency to change back to the original value, at a slower rate, however, than at room temperature.

The N type germanium sample exposed to a total of 4.37×10^{18} neutrons converted to P type but could not be completely healed out by heat treatment.[1] Using the new absorption cross section determined by H. Pomerance of the Physics Division, ORNL, it is possible to calculate the number and type of impurity atoms produced by neutron bombardment.

The number of transmutations N_t is given by:

$$N_t = nvt \ (2.05 \times 10^{-2}).$$

[1] We are indebted to Mr. J. R. Cleland of the Purdue semi-conductor group for the heat treatment, Hall effect, and resistivity measurement before and after bombardment and as a function of heat treatment.

* Consultant from Purdue University.

One would therefore expect about 9×10^{16} P type impurity centers corresponding to the total neutron flux of 4.37×10^{18} neutrons. The number found from Hall effect measurements is 6.2×10^{16}. This is in good agreement with the predictions since the cross sections are accurate only to 20% and the neutron flux is only a rough estimate.

The silicon sample exposed to a total of 2.62×10^{18} neutrons has become highly resistant material, and new evidence from infra-red measurements has been found at the Purdue semi-conductor laboratory for the existence of new levels at about .6 to .8 ev introduced by irradiation.

Scattering by Paramagnetic and Antiferromagnetic Materials (C. G. Shull, E. O. Wollan, W. A. Strauser). In the last quarterly report (ORNL 325 Supplement 1) experimental data on the scattering of neutrons by the paramagnetic substance MnO were given. It was reported there that the magnetic scattering was observable as a diffuse scattering superimposed on the regular crystalline pattern of Bragg reflections by nuclear scattering. Halpern and Johnson had predicted such a diffuse scattering along with an electronic form factor variation in angle, but the scattering data resembled a liquid or short range order type of scattering with a certain degree of coherence noticeable. It was suggested that this was to be interpreted as a short range or local coupling of the Mn^{++} permanent moments rather than a case of free and independent moments as considered in the theory of scattering by paramagnetic substances.

During the last period the scattering by two other Mn^{++} paramagnetic compounds ($MnSO_4$ and MnF_2) has been studied to see if the above coupling were present in these magnetically-more-dilute substances. The same procedure of data analysis and correction was followed as for MnO, with the results shown in Fig. 21. It is seen that there is much less evidence for local moment coupling in the sulphate and fluoride than in the oxide. The sulphate and fluoride data do not agree exactly and this may represent slight residual coupling effects or may be instrumental in nature since the sulphate data are less accurate because of lower intensities for measurement. In any event the scattering data for these two substances represent much more closely a true form factor decline in scattering cross section with angle as predicted for the scattering of independent moments. Data are now being obtained for MnF_2 at high temperature (400 - 500° C), where any residual coupling will be considerably lessened, so as to get the true magnetic form factor.

It has also been brought to our attention that the magnetic susceptibility data for MnO suggests an antiferromagnetic Curie temperature at 120° K below which neighboring magnetic moments are locked antiparallel to each other. This contrasts to the case of a ferromagnetic Curie temperature, below which the moments are locked parallel to each other. If such were true for MnO, then interesting coherent scattering effects should show up at low temperatures. Accordingly, MnO was studied at 80° K, considerably below the suggested Curie temperature, and the pattern is shown in Fig. 22 along with the room temperature pattern for comparison. It is seen that strong coherent magnetic effects are

UNCLASSIFIED
DWG. 7358

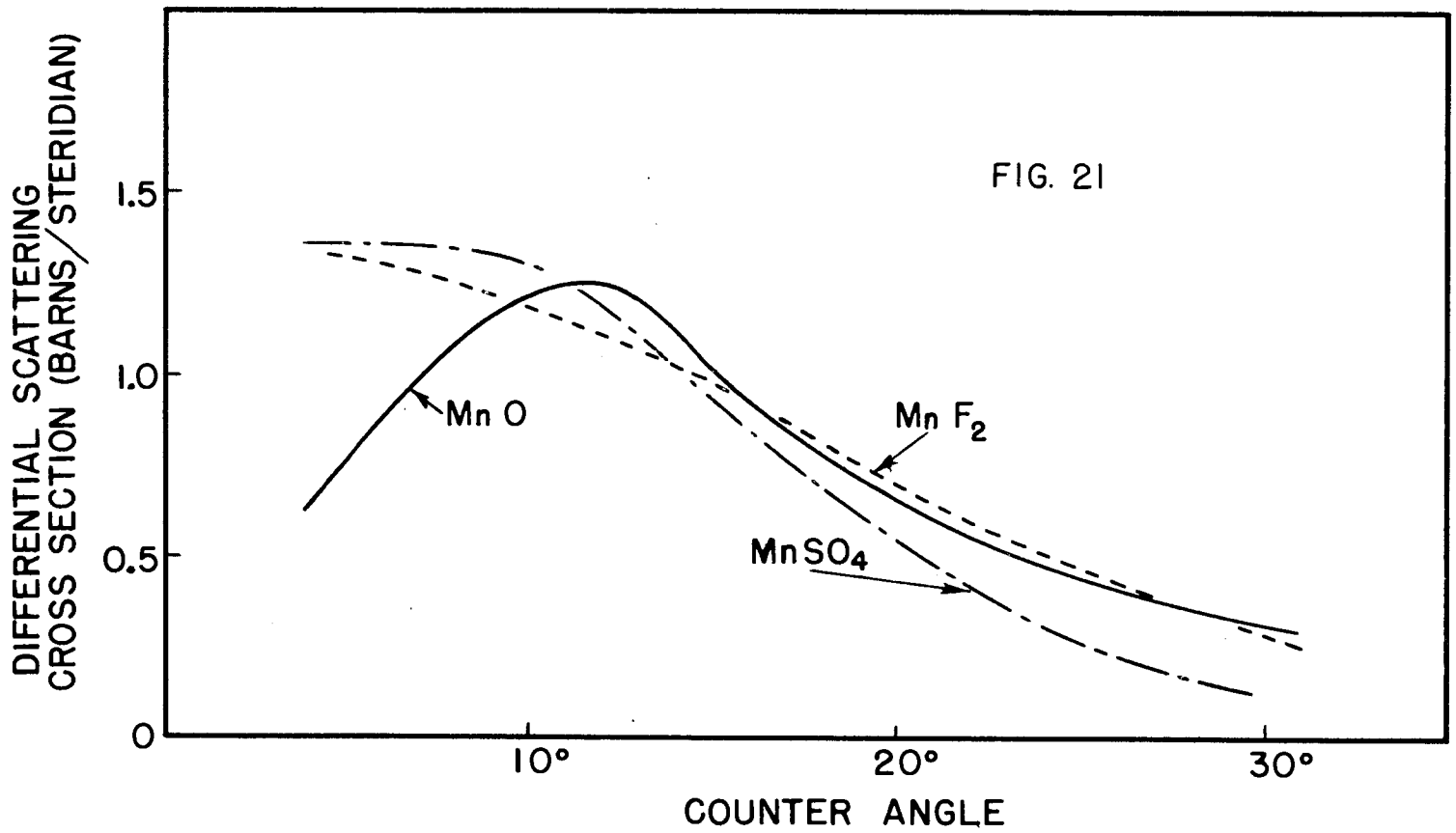

FIG. 21

UNCLASSIFIED
DWG. 7355

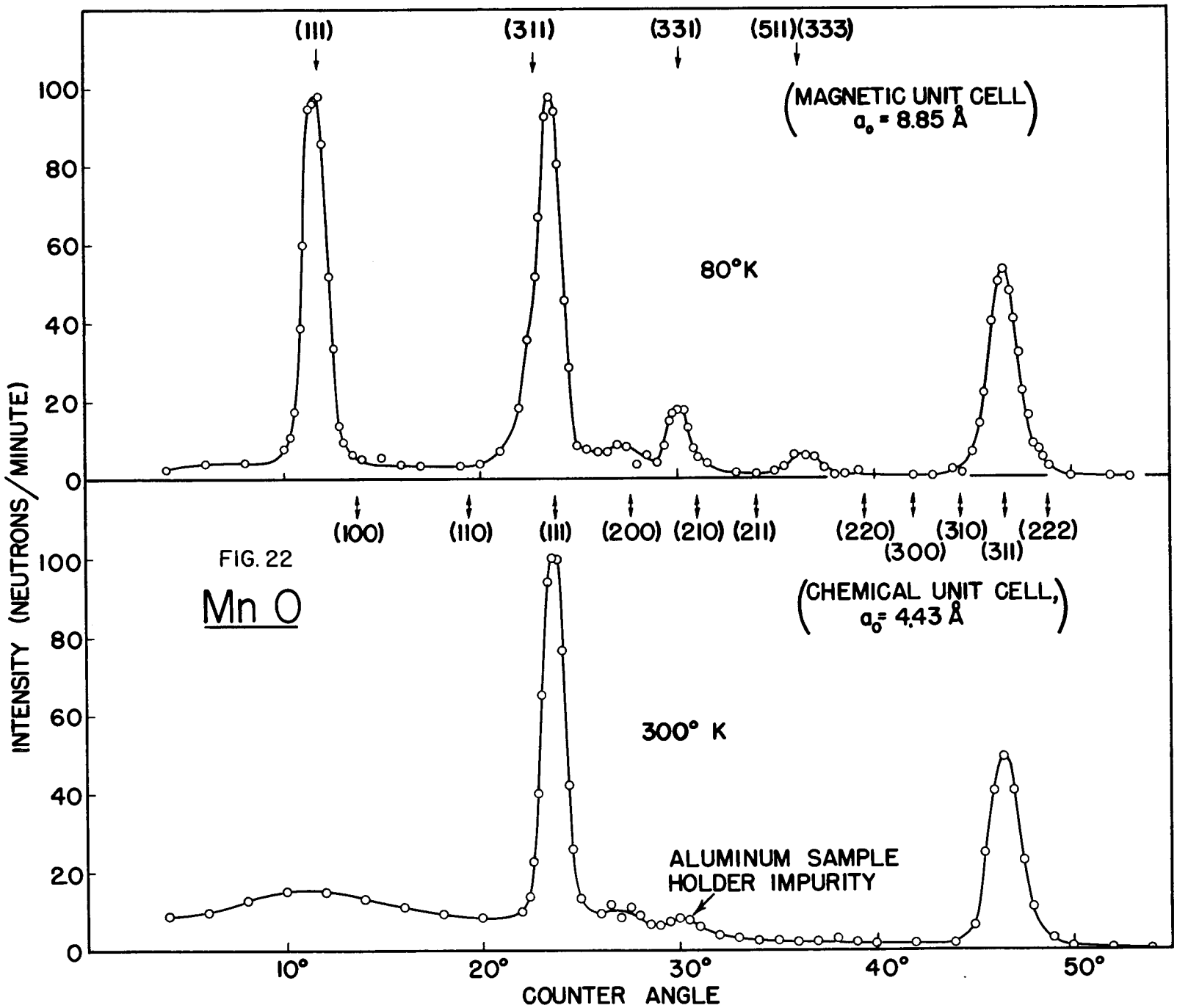

FIG. 22

Mn O

now present. Perhaps the most striking thing about the low temperature pattern is that the magnetic peaks do not fall at allowed reflection positions on the basis of the chemical unit cell. A crystallographic phase change cannot account for this since X-ray measurements below and above this temperature have shown the same chemical unit cell with slight change in spacing value. The magnetic peaks in the neutron pattern can be indexed, however, on the basis of a double size unit cell (eight times the original unit cell volume). For this magnetic unit cell the observed reflections are (111), (311), (331) and (511) as shown on the figure. This means that Mn atoms displaced by one chemical unit cell dimension (4.426 Å) from each other are scattering neutrons differently and hence the repeating distance is twice this value or 8.852 Å.

The intensities of the four detectable magnetic peaks have been evaluated and it is found that they fall off in intensity with angle just as the magnetic form factor suggested in Fig. 21. Thus they must be characterized by a common magnetic crystal structure factor. Since the amplitude of magnetic scattering is known both by calculation and by experiment, it is possible to evaluate the number of Mn atoms which are contributing to the observed intensity of scattering. When this is done it is found that the intensity can be accounted for by having only about one-fourth of the Mn atoms as effective scatterers. This may mean that the alignment of the atomic magnetic moments is such that only one-fourth of them are contributing to the scattering for an arbitrary axis of neutron moment alignment. A complete description of the magnetic structure is not available at this time and will be discussed at a later date.

Similar magnetic effects have been noticed in the pattern for α-Fe_2O_3 which is presumably antiferromagnetic at room temperature with an antiferromagnetic Curie temperature of 950° K. Extra peaks are found in the neutron pattern at room temperature which are not allowed on the basis of the chemical structure. Further studies are in order with this substance.

Neutron-Proton Scattering (C. G. Shull, E. O. Wollan, W. A. Strauser). For some time we have been planning to remeasure the coherent cross section for the scattering of neutrons by hydrogen. As is well known, the coherent scattering amplitude of hydrogen as determined from crystal diffraction together with the total free scattering amplitude of hydrogen permit an evaluation of the triplet and singlet amplitudes for n-p scattering from which conclusions can be drawn regarding the range of the neutron-proton interaction.

Work on this problem has been resumed but so far only preliminary results have been obtained. Some of the problems associated with this work are: (a) A pure sample of a hydrogen containing crystal must be obtained. (b) In a crystal such as NaH it is necessary, in the problem of obtaining an accurate value of the coherent amplitude of hydrogen, to determine the sodium coherent scattering amplitude by a study of some other sodium containing crystal. (c) Some reference standard must be available for which the coherent scattering cross section is known or can be accurately determined by direct transmission measurements. Diamond powder has been used for this standard and some other elements can be used. We are reinvestigating the accuracy with which these standard cross sections can be determined. (d) The temperature dependence of the coherent scattering by the hydrogen containing crystal in question must also be determined. There appears to be some uncertainty associated with the application of the Debye-Waller temperature factor to crystals having atoms which differ in mass by a rather large factor. To overcome this difficulty, the temperature dependence of NaH is being studied for both neutrons and X rays for which the relative scattering by the Na and H atoms are very different. This method promises to eliminate the uncertainties arising from this cause.

Recent preliminary measurements of the coherent scattering by NaH with the temperature factor determined as above, and with σ_{Na}^{coh} determined with NaF give results which agree closely with those previously reported *(Phys. Rev.* 73, 842 (1948).

Growing Large Crystals of Copper-Gold Alloy (F. A. Sherrill, M. A. Bredig). On request by E. O. Wollan and C. G. Shull, for application in their study of fundamental neutron diffraction effects, attempts were made to grow large single crystals of the ordered phase of Cu_3Au by the Bridgeman method in the vacuum furnace mentioned in the preceding quarterly report[1]. Crucibles of high purity graphite, 8 in. long, $\frac{1}{2}$ in. i.d., and pointed at the bottom, were employed. A slow rate of cooling the melt, which previously had been remelted twice and homogenized for 20 hours in the molten state, was provided by lowering the crucible out of the heating zone at the rate of 0.9 in. per hour. Quality and orientation of the crystals thus obtained were examined by means of X-ray back-reflection laue patterns. Wafers were cut parrallel to the (100) and (110) planes of the cubic lattice. Both X-ray patterns and etching with $FeCl_3$ solution revealed the presence, in most cases, of more than one crystal grain, which were aligned in more or less similar orientation. No improvement was obtained by annealing these aggregates for 6-8 hours at 800° C. The

[1]This furnace was designed by W. E. Johnson.

difficulties in growing good crystals of this alloy may be related to the separation of the solidus and liquidus curves in the melting diagram of the system copper-gold.

Neutron Activation Studies with Fast Pneumatic Tube (E. C. Campbell, K. L. Robertson). A new activity in lead having a half-life of the order of one second has been found. Since it is found in several different samples of high purity, as well as in ordinary lead, it is unlikely that the activity is due to an impurity. In an attempt to identify which isotope of lead is responsible for the activity, a small sample (24.5 mg) of $PbCrO_4$ isotopically enriched in Pb^{204} by a factor of 10 was exposed. The short period activity was not detected in any of several runs with this sample. From control runs with larger amounts of normal $PbCrO_4$ it was evident that if Pb^{204} were responsible, it should have been easily detectable. Additional samples will be tested to decide this question.

Absorption measurements in lead and aluminum show that the radiation associated with this activity is rather penetrating. The results obtained so far indicate a gamma ray of at least 0.5 Mev and a softer component of 2 Mev beta rays.

Cadmium Capture γ-Rays (C. D. Moak and J. W. T. Dabbs). In the last quarterly report a preliminary block diagram of the final run for Cd was presented. The run has been completed and the results are given here.

Figure 23-a is a plot of the distribution of the 208 pairs observed in the final run. Figure 24-a is the capture γ-ray spectrum for these pairs obtained by dividing 23-a by the pair-production cross section. Except at the ends of the curves, the probable error for 23-a and 24-a is held at 13%. Vertical lines drawn along 23-a illustrate the size of the error.

Previous work yielded data which were unreliable below 3.75 Mev. Above that energy the data of 23-a have been added to those of previous runs and area-normalized to join with 23-a at 3.75 Mev, giving the curve 23-b. Dividing 23-b by pair-production cross section gave the curve 24-b. Except at the ends of the curves, 23-b and 24-b have a probable error of 9.5%.

Spurious effects make the curves 23-a and 24-a unreliable below 2 Mev.

The data seem to indicate that the maximum energy of the capture γ-rays from Cd is considerably above 7 Mev.

Pile Oscillator (H. Pomerance). Table 1 gives a summary of the thermal neutron capture cross sections of the 69 elements as measured up to date with the ORNL pile oscillator. Five of these elements have capture resonances at

NOT CLASSIFIED
DWG. 7354

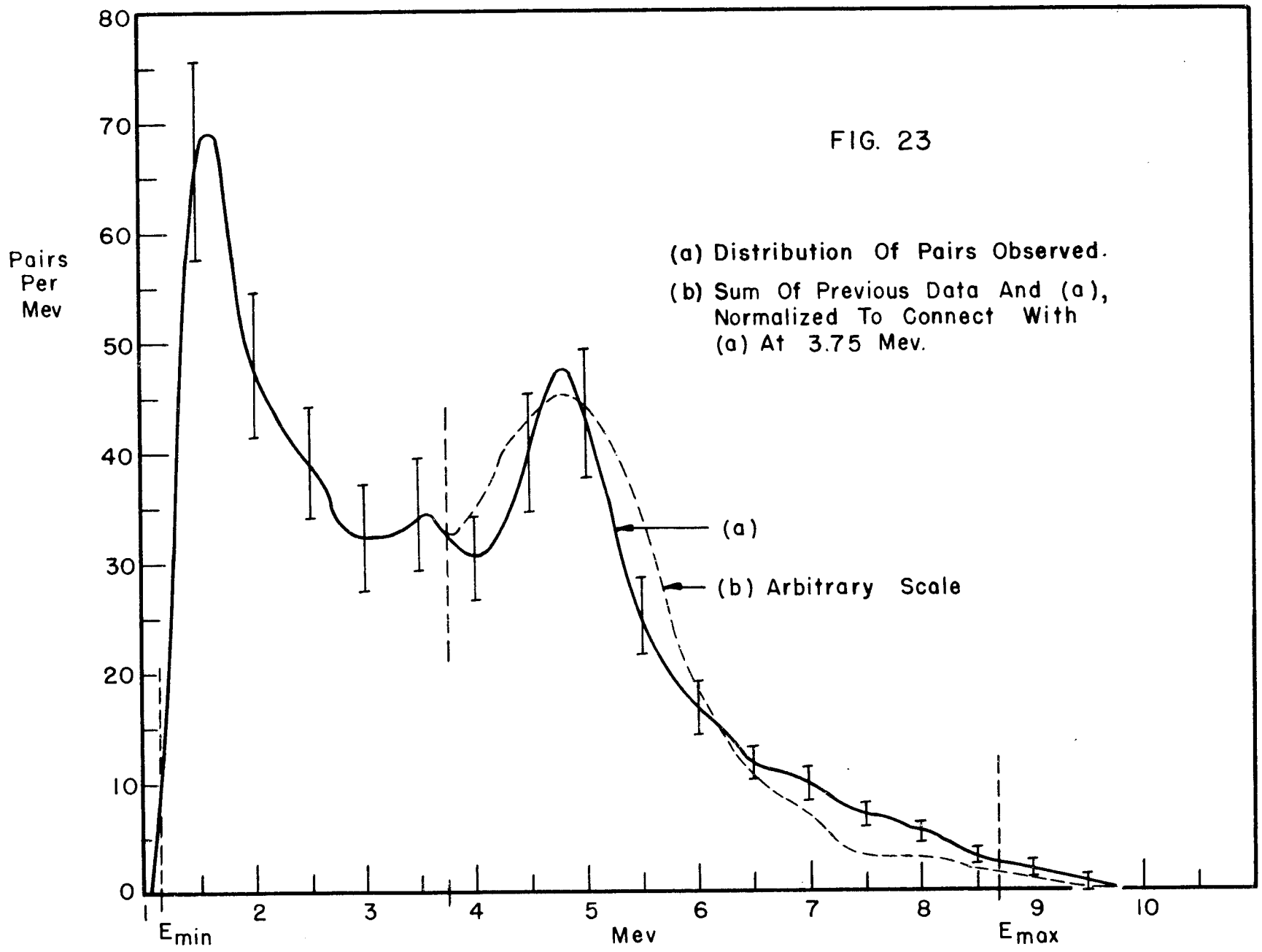

FIG. 23

(a) Distribution Of Pairs Observed.

(b) Sum Of Previous Data And (a), Normalized To Connect With (a) At 3.75 Mev.

NOT CLASSIFIED
DWG. 7357

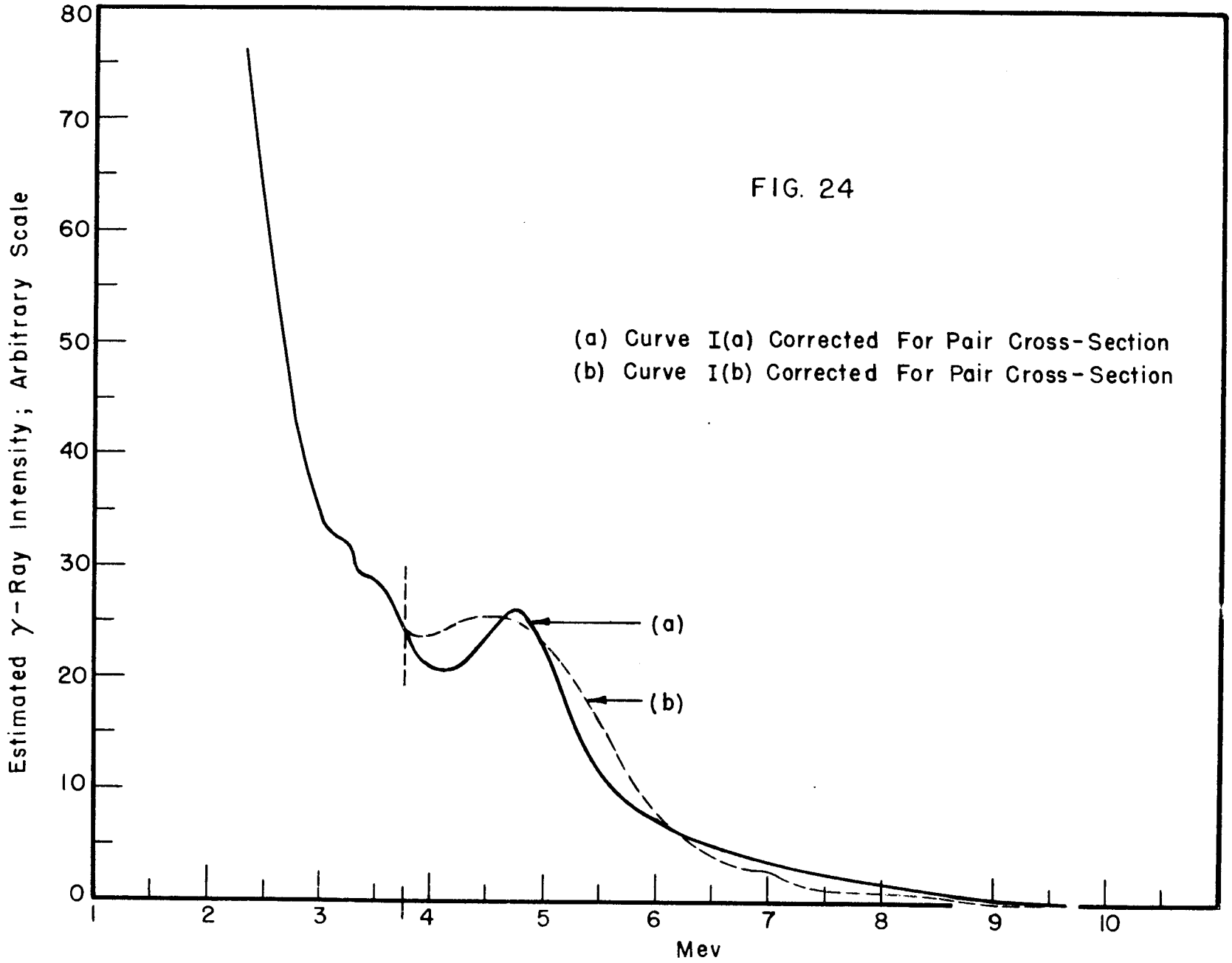

FIG. 24

(a) Curve I(a) Corrected For Pair Cross-Section
(b) Curve I(b) Corrected For Pair Cross-Section

thermal energies and are marked by an "r" to indicate that the cross sections are an average over the pile neutron spectrum. For four elements more work needs to be done for the best attainable accuracy, and the tentative values listed in the table are marked by an asterisk. The values of the capture cross sections in the table were obtained by comparison with gold, 95 barns being taken as the gold capture cross section at thermal energy (0.025 ev).

TABLE 1

THERMAL NEUTRON CAPTURE CROSS SECTIONS OF 69 ELEMENTS AS MEASURED WITH THE PILE OSCILLATOR

AT. NO.	ELEMENT	σ_c	AT. NO.	ELEMENT	σ_c
3	Lithium	66.9 b	31	Gallium	2.77 b
7	Nitrogen	1.86	32	Germanium	2.31
11	Sodium	0.46	33	Arsenic	4.14
12	Magnesium	0.06	34	Selenium	12.1
13	Aluminum	0.22	35	Bromine	6.4*
14	Silicon	0.09	37	Rubidium	0.70
15	Phosphorus	0.15	38	Strontium	1.16
16	Sulfur	0.47	39	Yttrium	1.38
17	Chlorine	32.7	40	Zirconium	0.35*
19	Potassium	2.05	41	Columbium	1.06
20	Calcium	0.41	42	Molybdenum	2.40
21	Scandium	11.8	44	Ruthenium	2.46
22	Titanium	5.83	45	Rhodium	150.
23	Vanadium	4.72	46	Palladium	6.6
24	Chromium	2.83	47	Silver	59.6
25	Manganese	12.8	48	Cadmium	3300. (r)
26	Iron	2.39	49	Indium	191.2
27	Cobalt	34.2	50	Tin	0.57
28	Nickel	4.49	51	Antimony	5.26
29	Copper	3.66	52	Tellurium	4.53
30	Zinc	1.00	53	Iodine	6.06

TABLE 1 (cont'd.)

AT. NO.	ELEMENT	σ_c	AT. NO.	ELEMENT	σ_c
55	Cesium	28.9 b	70	Ytterbium	35.7 b
56	Barium	1.05	71	Lutecium	108.
57	Lanthanum	8.8	72	Hafnium	103.
58	Cerium	0.65	73	Tantalum	21.3
59	Praseodymium	11.2	74	Tungsten	17.7
60	Neodymium	44.9	75	Rhenium	83.9
62	Samarium	10400. (r)	76	Osmium	14.7
63	Europium	3600. (r)	77	Iridium	464. (r)
64	Gadolinium	35000. (r)	78	Platinum	9.*
65	Terbium	55.*	79	Gold	95.0
66	Dysprosium	892.	80	Mercury	341.
67	Holmium	66.6	81	Thallium	3.29
68	Erbium	166.	82	Lead	0.191
69	Thulium	118.			

*Theses values are tentative pending further work.

NUCLEAR PHYSICS AND LOW TEMPERATURES

Low Temperature Program (L. D. Roberts, J. W. T. Dabbs and J. K. Leslie). The low temperature program at ORNL is still in a stage of equipment installation and testing, but some preliminary experiments have been started.

The installation of the large electromagnet, mentioned in the last quarterly report, has just been completed and we are now in the process of making preliminary tests of this equipment. All of the associated equipment necessary to obtain temperatures of approximately .01° K (Dewar flasks, electronic instrumentation, and high vacuum equipment) have been assembled and are now being installed.

One of the primary purposes of the low temperature program here is to align nuclei at very low temperatures by an intense magnetic field. To accomplish this, one must transfer heat from the sample of material containing the nuclei to the refrigerant chrome alum used to obtain the low temperature.

This involves making a thermal contact between the refrigerating salt and a copper or silver bar used to conduct the heat. We are studying various techniques of making this thermal contact, and, in support of this program, we are measuring a number of thermal coefficients of expansion from room temperature down to 4° K. We are also studying the possible use of the rare earth metals or their alloys as refrigerants in adiabatic demagnetizations. One material, an alloy of cerium and magnesium, has been investigated in a very preliminary way and has been found to be unsuitable. It is hoped, however, that a further study of the rare earth metals and their alloys will reveal a suitable system.

Cross Section of He^3 as a Function of Energy (T. E. Stephenson). It is planned to measure the neutron cross section of He^3 as a function of neutron energy. The energy range to be covered is from about 0.03 ev to about 0.5 ev and thus will extend the work reported by King and Goldstein.[2]

A vacuum system has been constructed for the transfer of the helium^{-3} from its present container to one suitable for use in cross section measurements. Actual transfer will be accomplished with a Toepler pump. At the present time a vacuum of about 10^{-4} mm of mercury has been attained and "dry run" or practice transfers are being made. Improvements in the system will be made. Appreciation is expressed to Dr. L. D. Roberts for his advice and help in constructing the vacuum system.

[2] L. P. King, Louis Goldstein, "The total cross section of the He^3 nucleus for slow neutrons," *Phys. Rev.*, **75**, 1366 (1949).

The cross section will be determined by the transmission method. It is currently planned to use the same arrangement in taking measurements as was used in determining the cross section of small samples of erbium, hafnium, Ni^{58} and Ni^{60}. The gas will be collected in a steel cylinder about 3 in. long and about 2 mm inner diameter. This tube, and an empty duplicate, will be shifted alternately into and out of the neutron beam. The beam, near the center of the pile, is about 16 sq in. in area and is caused to coverage by tapered graphite stringers so that at a point about five ft from the outer pile face, the beam will be defined by the walls of the steel cylinder. After passing through the cylinder, the beam is allowed to diverge by tapered graphite stringers so that upon emerging from the pile shielding the beam is about one square inch in area. Mono-energetic neutrons are selected and counted with the bent crystal neutron spectrometer.

VAN DE GRAAFF

Van de Graaff (W. Good, R. Lamphere, F. Rink, R. Bennett). During last quarter, progress has been made (a) on the accelerator tube, (b) the ion source, (c) the pumping problem, and (d) voltage production and control.

Accelerator Tube. Details of the accelerator tube decided upon include dimensions on the insulators composing the tube, and the shapes of the accelerating electrode. The insulators are of pyrex glass to be cut to the specified dimensions, and the electrodes are of stainless steel. Dimensions have been chosen to achieve the largest possible pumping speed, the outside diameter of the tube being limited by the space allowed for it in the Van de Graaff generator. A few insulators and electrodes have been fabricated for the purpose of making a test section of tube. The test section will be used to study the behavior of the glass and seals under operating conditions. Experience shows that an accelerator tube has to be "aged." That is, the maximum voltage a tube will stand increases to a limit, with time of applied voltage. Apparatus for this conditioning is under way.

Ion Source. The previous report stated that an ion source of the type described by Oppenheimer R.S.I. 20, 189 (1949) had been built. This ion-source has delivered through a 2 mm hole from the differential pumping chamber, currents amounting to 170 microamperes at 20 KEV with a gas flow rate of about 20 cc/hr into the gas chamber. However, difficulty has been encountered in getting anything but a micro-ampere or so of analyzed beam in the collector cap. This is presumably due to lack of proper alignment of source, aperatures, and analyzer, so that most of the beam is being lost to the analyzer walls. This condition is being corrected.

Due to the temperatures attained by the pyrex glass envelope constituting the arc chamber, considerable difficulty has been encountered with excessive conductivity. This problem arises because the design of ion-source is characterized by an axial magnetic field of 1000 gauss or more in the ionizing region. This field is supplied by a solenoid surrounding the discharge region. Heat is supplied to the glass walls of the arc chamber principally by the filament in the arc source. This heat is improperly dissipated because of the surrounding solenoid which actually contributes more heat. To obviate, even temporarily, the difficulties due to glass leakage, the glass tube has been

water cooled, and alternatively replaced by lavite. The latter material, however, is naturally too porous for vacuum operation and a suitable glaze has not been found. The biggest improvement has been the substitution of an oxide-coated filament for the pure tungsten one, thereby permitting the power input to the electron emitter to be greatly reduced. In this manner the source can be operated several hours before break down occurs over the glass. The use of quartz in place of the pyrex may be necessary.

Pumping Problem. The problem of pumping at the *top* is continuing to be tackled both by the brute force method of diffusion plus mechanical pumps and in the case of hydrogen and deuterium by getter action.

An attempt has been made to modify the VMF-260 Oil Diffusion Pump so as to stand the 200 lb external pressure. However, to date, the welding has not been satisfactory. The commercial NCR Type H-2 Series A is being studied to see if it will meet the requirements, before further attempts are made to make the VMF-260 perform. A Duo-Seal Model-1400 is the fore pump selected as most readily modified to meet the exterior pressure requirements. A special diffusion-pump, trap and baffle are under construction, the purpose of which is to keep the oil in the accelerator tube to our absolute minimum.

Numerous suggestions have been made as to the possible use of uranium as a getter for hydrogen through the formation of uranium hydride (UH_3). It has been shown, *Nucleonics* 4,4 (1949), that for uranium hydride,

$$\log_{10} p_{dec} = -\frac{4500}{T} + 9.28$$

where p_{dec} = decomposition pressure in mm of Hg at absolute temperature T. This relation was obtained in the region 200 to 400° C. Extrapolating this result to 40° C gives

$$p_{dec} = \text{ultimate vacuum at } 40^\circ \text{ C} = 8 \times 10^{-6} \text{ mm Hg.}$$

No data were given from which the pumping rate per gram of activated uranium could be inferred or estimated. Studies to be described at some future time have shown that at room temperature, 200 grams of activated uranium will absorb gas at a rate

$$\frac{dQ}{dt} = 21.3(p - .038),$$

where Q is measured in μ liter (at atmospheric pressure) and p is measured in microns of Hg. Thus at 10^{-4} mm Hg, 200 grams of activated uranium provides a

pumping speed of about 15 l/sec. This result is promising and further studies are proceeding on uranium as well as on other possible getters.

Voltage Production and Control. Further work has been done to evaluate CO_2 as a possible insulating gas. Reference has been made in past reports to the fact that CO_2 with a contamination of sulfur hexafluoride had something like twice the break down gradient that air has at the same pressure.

Volt-ampere characteristics for point to plane discharge have been investigated for pressures in the range 0 - 300 lbs gauge with spacings from 1 to 6 mm. Negative point-to-plane corona is stable, but positive point-to-plane exhibits considerable instability above 150 lbs. This is similar to the behavior of nitrogen. The general tendency of gases to exhibit positive point-to-plane corona instability at high pressures can probably be compensated by some type of current limiting device in the spray supply.

SHIELDING

Capture Gamma Ray Studies (N. F. Lansing, E. P. Blizard). Work has continued on the development of techniques for the use of deuterium loaded photographic emulsions to determine capture gamma ray energies. Efforts are being made to establish quantitative relations between the observed track distributions and such variables as development delay at various temperatures and various details of development technique. There are definite indications that the latent images of tracks in water soaked emulsions tend to fade if the plates are permitted to remain at room temperature for as long as 20 hours between the times of exposure and development.

Summer Work Session on Shielding (E. P. Blizard). A three month study session has been organized to plan shielding work for the coming year, to evaluate work done to date, and to advance the state of the art where possible. Specifically the following items are expected to be included in the final report:

1. A program of experiments for the ORNL lid tank shield-testing facility.

2. An evaluation of theoretical work to date, so that shield designs can be made with more assurance. It is anticipated that T. A. Welton, on contract with AEC, will take the prime responsibility for this section.

3. A program for computing machinery, including some smaller problems which will aid in understanding the relative importance of the various attenuation processes.

THEORETICAL PHYSICS

Theoretical Physics (M. E. Rose). Most of the past three months has been devoted to planning the L-shell internal conversion calculations. Investigations of various questions such as relative contribution of the three sub-shells, importance of relativistic effects for the three sub-shells, and relative importance of screening and obtaining screened fields are under way. Attempts have been made to simplify the work since it appears that the L-shell conversion will constitute one of the most formidable problems ever put on the automatic computing machines. So far all of the simplifying procedures considered have been rejected for one of several reasons. Those which involve some approximation based on physical ideas incur an error which is difficult to estimate without such extensive computations that their advantage would be dubious. Other procedures which have been considered would eliminate some of the laborious parts of the calculation but would involve new difficulties. Thus far, the straightforward "hammer and tongs" attack seems most feasible. Some of the uncertainties as to procedure stem from the fact that it has not been decided on what machine these computations can be done in a reasonable way.

NEUTRON DECAY

Neutron Decay Experiment (F. Pleasonton, R. V. McCord, A. H. Snell). In our last report (ORNL 325, Supplement 1) we gave tentative results of our search for beta-proton coincidences arising from neutron decay. These results were taken as indicative only, inasmuch as the beta counters were known to be functioning poorly. We have now changed from Geiger to beta-proportional counters, and have obtained great improvement in reproducibility of counts and in the lifetime of the counters. The result of three weeks of coincidence counting are given in Table 1.

A brief recapitulation may be necessary to make the table intelligible. Coincidences are sought within a resolving time of 1.4 μ-sec between counts in the two-celled beta proportional counter AB, and a secondary electron multiplier which is arranged so as to count the focused and accelerated protons. In effect, triple coincidences are measured; *viz.*, coincidences between the multiplier pulses and pulses from cell A and cell B of the beta counter. To see if such coincidences behave as they should if they originate from decaying neutrons, a study is made of the effect of (1) removing slow neutrons from the beam by interposing a B^{10} shutter ahead of the apparatus, (2) placing a thin foil (sufficient to stop the protons) over the entrance to the multiplier, and (3) removing the electric field which accelerates and focuses the protons onto the multiplier. Thus we establish what we call boron differences, foil differences, and voltage differences. If there is a genuine neutron decay effect, the boron difference taken with foil open and voltage on should have a positive value, and it should equal the foil difference taken with the boron out and the voltage on, and the voltage difference taken with the foil open and the boron out. All other combinations of boron, foil and voltage settings (e.g. the boron difference with foil closed and voltage either on or off) should give differences of zero.

The figures in Table 1 give the various boron, voltage and foil differences in counts per minute in excess of the random rates. The latter were separately measured in a separate counting channel. Thus the first figure in the table is derived as follows:

$$\{(\text{Genuine} + \text{random}) - \text{random}\}_{\text{Boron out}} - \{(\text{Genuine} + \text{random}) - \text{random}\}_{\text{Boron in}}$$

or in actual counts per minute,

$$\{(3.04 \pm .06) - (1.88 \pm .05)\} - \{(1.51 \pm .03) - (1.14 \pm .04)\} = 0.79 \pm .09.$$

All of the other differences are derived from experimental counting rates in the same realm of magnitude.

TABLE 1

1.	Boron difference with foil open, voltage on	0.79 ± .09 cpm
2.	Boron difference with foil open, voltage off	0.00 ± .08
3.	Boron difference with foil closed, voltage on	0.08 ± .06
4.	Boron difference with foil closed, voltage off	0.11 ± .07
5.	Foil difference with boron out, voltage on	0.80 ± .09
6.	Foil difference with boron out, voltage off	-0.15 ± .08
7.	Foil difference with boron in, voltage on	0.09 ± .06
8.	Foil difference with boron in, voltage off	-0.04 ± .06
9.	Voltage difference with boron out, foil open	0.89 ± .10
10.	Voltage difference with boron out, foil closed	-0.06 ± .08
11.	Voltage difference with boron in, foil open	0.10 ± .06
12.	Voltage difference with boron in, foil closed	-0.03 ± .06

A glance at Table 1 shows that there is indeed an effect that could well originate from decaying neutrons. The three differences given on lines 1, 5 and 9 are finite and equal within statistical error, whereas all of the other differences are essentially zero. When we take into account the fact that these data are experimentally of much better quality than any we have previously obtained, we can only conclude that either neutrons do indeed decay, or else by some improbable circumstance the differences of lines 1, 5 and 9 come out to be finite and equal in spite of the varied nature of the manipulations which gave rise to them.

As a further check on the dependence of these effects upon the presence of neutrons, we have sought foil and voltage differences with the pile off, and with a pure gamma source (Co^{60}) placed at the point where the neutrons enter the vacuum chamber. The coincidence counting rates are low, and the time with the pile off is restricted; consequently the statistics so far are poor. The results, however, are given in Table 2.

TABLE 2

13. Foil difference with voltage on:	-0.10 ± .07 cpm
14. Foil difference with voltage off:	0.08 ± .06
15. Voltage difference with foil open:	0.03 ± .07
16. Voltage difference with foil closed:	0.15 ± .07

Boron differences of course have no significance here. These differences were derived from raw counting data as, for example, that for line 13:

$$\{(\text{Genuine} + \text{random}) - \text{random}\}_{\text{Foil open}} - \{(\text{Genuine} + \text{random}) - \text{random}\}_{\text{Foil closed}}$$

$$\{(0.65 \pm .04) - (0.51 \pm .03)\} - \{(0.61 \pm .04) - (0.37 \pm .03)\}$$

$$= 0.10 \pm .07 \text{ cpm}$$

Although the absolute counting rates are only about half of those from which the differences of Table 1 were derived, it is nevertheless clear that lines 13 and 15 do not show a positive effect comparable with lines 5 and 9. We conclude that pure gamma rays do not produce foil and voltage differences in the coincidence rates. The presence of the beam from the pile seems to be required.

In order to derive a value of the half-life of the neutron from the coincidence readings of Table 1, we have obtained the effective solid angle for the AB counter by placing a calibrated* beta source of Te^{204} at various points in a mocked-up three-dimensional geometry. Assuming from Table 1 that 0.83 counts per minute are obtained from decaying neutrons, we obtain:

No. of neutrons decaying per minute

$$= 0.83 \times \frac{1}{\text{Solid angle of AB counter}} \times \frac{1}{\text{Multiplier collecting efficiency}}$$

$$\times \frac{1}{\text{Multiplier bias factor}}$$

$$= 0.83 \times \frac{1}{0.32 \times 10^{-2}} \times \frac{1}{0.60} \times \frac{1}{0.33}$$

$$= 1300.$$

* We are indebted to C. Borkowski of the Chemistry Division for the absolute calibration of this source.

To obtain the number of neutrons present in the sample under examination, we have used an improved method whereby a thin gold foil is stretched completely across the beam, and activated*. This avoids a separate evaluation of the geometrical cross section, as was needed previously when a small (1 cm^2) foil was activated. Taking cadmium differences, this gave $\int nds = 4.7 \times 10^4$ neutrons, where n is the number of neutrons per cc at the surface element ds, and the integral is taken over the cross section of the beam. Multiplying by the effective length of the beam from which counts are taken, we obtain 33,000 for the number of neutrons in the sample. Thus, we obtain for the neutron,

$$T_{\frac{1}{2}} = \frac{33,000 \times 6.93}{1300}$$

$$= 18 \text{ min.}$$

The estimated uncertainty is about 25%.

In conclusion, we can state that our observations are in agreement with the supposition the neutrons undergo radioactive decay with emission of beta particles, and that the associated half-life is very probably in the interval 10-30 min.

* We are greatly indebted to R. A. Brosi of the Chemistry Division for help in measuring these foils. The whole foil was placed in Brosi's gamma ionization chamber for measurement, and the ionization chamber was calibrated with another gold foil which has been counted absolutely with Brosi's coincidence apparatus.